

International Energy Agency, EBC Annex 58

# Reliable building energy performance characterisation based on full scale dynamic measurements

**Report of Subtask 1b:  
Overview of methods to analyse dynamic data**

Arnold Janssens





International Energy Agency, EBC Annex 58

# Reliable building energy performance characterisation based on full scale dynamic measurements

## Report of Subtask 1b: Overview of methods to analyse dynamic data

### Author

Ghent University, Gent, Belgium (<http://www.architectuur.ugent.be/en>)

Arnold Janssens

With contributions from:

Giuseppina Alcamo (UniFi), Peder Bacher (DTU), Geert Bauwens (KU Leuven), Aitor Erkoreka (UPV/EHU), Gilles Flamant (BBRI), Christian Ghiaus (INSA), Eline Himpe (UGent), Arnold Janssens (UGent), Maria-José Jiménez (CIEMAT), David Johnston (Leeds-Beckett), Guillaume Pandraud (Isover-Saint Gobain), Samuel Stamp (UCL).

Reviewed by:

Matthias Kersken (Fraunhofer IBP), Staf Roels (KU Leuven), Linda Xiao Fu (Hong Kong PolyU)

© Copyright KU Leuven, Belgium 2016

All property rights, including copyright, are vested in KU Leuven, Belgium, Operating Agent for EBC Annex 58, on behalf of the Contracting Parties of the International Energy Agency Implementing Agreement for a Programme of Research and Development on Energy in Buildings and Communities. In particular, no part of this publication may be reproduced, stored in a retrieval system or transmitted in any form or by any means, electronic, mechanical, photocopying, recording or otherwise, without the prior written permission of KU Leuven.

Published by KU Leuven, Belgium

Disclaimer Notice: This publication has been compiled with reasonable skill and care. However, neither KU Leuven nor the EBC Contracting Parties (of the International Energy Agency Implementing Agreement for a Programme of Research and Development on Energy in Buildings and Communities) make any representation as to the adequacy or accuracy of the information contained herein, or as to its suitability for any particular application, and accept no responsibility or liability arising out of the use of this publication. The information contained herein does not supersede the requirements given in any national codes, regulations or standards, and should not be regarded as a substitute for the need to obtain specific professional advice for any particular application.

ISBN: 9789460189890

Participating countries in EBC:

Australia, Austria, Belgium, Canada, P.R. China, Czech Republic, Denmark, Finland, France, Germany, Greece, Ireland, Italy, Japan, Republic of Korea, the Netherlands, New Zealand, Norway, Poland, Portugal, Spain, Sweden, Switzerland, Turkey, United Kingdom and the United States of America.

Additional copies of this report may be obtained from:

[www.iea-ebc.org](http://www.iea-ebc.org)

[essu@iea-ebc.org](mailto:essu@iea-ebc.org)

*cover picture: Tailored heating experiment performed for one of the industrial partners of the Annex 58-project to determine the overall heat loss coefficient of a newly built dwelling based on on-site measured data. (source: Geert Bauwens, KU Leuven)*

# Preface

## The International Energy Agency

The International Energy Agency (IEA) was established in 1974 within the framework of the Organisation for Economic Co-operation and Development (OECD) to implement an international energy programme. A basic aim of the IEA is to foster international co-operation among the 29 IEA participating countries and to increase energy security through energy research, development and demonstration in the fields of technologies for energy efficiency and renewable energy sources.

## The IEA Energy in Buildings and Communities Programme

The IEA co-ordinates international energy research and development (R&D) activities through a comprehensive portfolio of Technology Collaboration Programmes. The mission of the Energy in Buildings and Communities (EBC) Programme is to develop and facilitate the integration of technologies and processes for energy efficiency and conservation into healthy, low emission, and sustainable buildings and communities, through innovation and research. (Until March 2013, the IEA-EBC Programme was known as the Energy in Buildings and Community Systems Programme, ECBCS.)

The research and development strategies of the IEA-EBC Programme are derived from research drivers, national programmes within IEA countries, and the IEA Future Buildings Forum Think Tank Workshops. The research and development (R&D) strategies of IEA-EBC aim to exploit technological opportunities to save energy in the buildings sector, and to remove technical obstacles to market penetration of new energy efficient technologies. The R&D strategies apply to residential, commercial, office buildings and community systems, and will impact the building industry in five focus areas for R&D activities:

- Integrated planning and building design
- Building energy systems
- Building envelope
- Community scale methods
- Real building energy use

## The Executive Committee

Overall control of the IEA-EBC Programme is maintained by an Executive Committee, which not only monitors existing projects, but also identifies new strategic areas in which collaborative efforts may be beneficial. As the Programme is based on a contract with the IEA, the projects are legally established as Annexes to the IEA-EBC Implementing Agreement. At the present time, the following projects have been initiated by the IEA-EBC Executive Committee, with completed projects identified by (\*):

- Annex 1: Load Energy Determination of Buildings (\*)
- Annex 2: Ekistics and Advanced Community Energy Systems (\*)
- Annex 3: Energy Conservation in Residential Buildings (\*)
- Annex 4: Glasgow Commercial Building Monitoring (\*)
- Annex 5: Air Infiltration and Ventilation Centre
- Annex 6: Energy Systems and Design of Communities (\*)
- Annex 7: Local Government Energy Planning (\*)
- Annex 8: Inhabitants Behaviour with Regard to Ventilation (\*)
- Annex 9: Minimum Ventilation Rates (\*)
- Annex 10: Building HVAC System Simulation (\*)
- Annex 11: Energy Auditing (\*)
- Annex 12: Windows and Fenestration (\*)
- Annex 13: Energy Management in Hospitals (\*)
- Annex 14: Condensation and Energy (\*)
- Annex 15: Energy Efficiency in Schools (\*)

- Annex 16: BEMS 1- User Interfaces and System Integration (\*)
- Annex 17: BEMS 2- Evaluation and Emulation Techniques (\*)
- Annex 18: Demand Controlled Ventilation Systems (\*)
- Annex 19: Low Slope Roof Systems (\*)
- Annex 20: Air Flow Patterns within Buildings (\*)
- Annex 21: Thermal Modelling (\*)
- Annex 22: Energy Efficient Communities (\*)
- Annex 23: Multi Zone Air Flow Modelling (COMIS) (\*)
- Annex 24: Heat, Air and Moisture Transfer in Envelopes (\*)
- Annex 25: Real time HVAC Simulation (\*)
- Annex 26: Energy Efficient Ventilation of Large Enclosures (\*)
- Annex 27: Evaluation and Demonstration of Domestic Ventilation Systems (\*)
- Annex 28: Low Energy Cooling Systems (\*)
- Annex 29: Daylight in Buildings (\*)
- Annex 30: Bringing Simulation to Application (\*)
- Annex 31: Energy-Related Environmental Impact of Buildings (\*)
- Annex 32: Integral Building Envelope Performance Assessment (\*)
- Annex 33: Advanced Local Energy Planning (\*)
- Annex 34: Computer-Aided Evaluation of HVAC System Performance (\*)
- Annex 35: Design of Energy Efficient Hybrid Ventilation (HYBVENT) (\*)
- Annex 36: Retrofitting of Educational Buildings (\*)
- Annex 37: Low Exergy Systems for Heating and Cooling of Buildings (LowEx) (\*)
- Annex 38: Solar Sustainable Housing (\*)
- Annex 39: High Performance Insulation Systems (\*)
- Annex 40: Building Commissioning to Improve Energy Performance (\*)
- Annex 41: Whole Building Heat, Air and Moisture Response (MOIST-ENG) (\*)
- Annex 42: The Simulation of Building-Integrated Fuel Cell and Other Cogeneration Systems (FC+COGEN-SIM) (\*)
- Annex 43: Testing and Validation of Building Energy Simulation Tools (\*)
- Annex 44: Integrating Environmentally Responsive Elements in Buildings (\*)
- Annex 45: Energy Efficient Electric Lighting for Buildings (\*)
- Annex 46: Holistic Assessment Tool-kit on Energy Efficient Retrofit Measures for Government Buildings (EnERGo) (\*)
- Annex 47: Cost-Effective Commissioning for Existing and Low Energy Buildings (\*)
- Annex 48: Heat Pumping and Reversible Air Conditioning (\*)
- Annex 49: Low Exergy Systems for High Performance Buildings and Communities (\*)
- Annex 50: Prefabricated Systems for Low Energy Renovation of Residential Buildings (\*)
- Annex 51: Energy Efficient Communities (\*)
- Annex 52: Towards Net Zero Energy Solar Buildings (\*)
- Annex 53: Total Energy Use in Buildings: Analysis & Evaluation Methods (\*)
- Annex 54: Integration of Micro-Generation & Related Energy Technologies in Buildings (\*)
- Annex 55: Reliability of Energy Efficient Building Retrofitting - Probability Assessment of Performance & Cost (RAP-RETRO) (\*)
- Annex 56: Cost Effective Energy & CO2 Emissions Optimization in Building Renovation
- Annex 57: Evaluation of Embodied Energy & CO2 Equivalent Emissions for Building Construction
- Annex 58: Reliable Building Energy Performance Characterisation Based on Full Scale Dynamic Measurements
- Annex 59: High Temperature Cooling & Low Temperature Heating in Buildings
- Annex 60: New Generation Computational Tools for Building & Community Energy Systems
- Annex 61: Business and Technical Concepts for Deep Energy Retrofit of Public Buildings
- Annex 62: Ventilative Cooling
- Annex 63: Implementation of Energy Strategies in Communities
- Annex 64: LowEx Communities - Optimised Performance of Energy Supply Systems with Exergy Principles
- Annex 65: Long Term Performance of Super-Insulating Materials in Building Components and Systems
- Annex 66: Definition and Simulation of Occupant Behavior Simulation
- Annex 67: Energy Flexible Buildings
- Annex 68: Design and Operational Strategies for High IAQ in Low Energy Buildings

Annex 69: Strategy and Practice of Adaptive Thermal Comfort in Low Energy Buildings  
Annex 70: Energy Epidemiology: Analysis of Real Building Energy Use at Scale

Working Group - Energy Efficiency in Educational Buildings (\*)  
Working Group - Indicators of Energy Efficiency in Cold Climate Buildings (\*)  
Working Group - Annex 36 Extension: The Energy Concept Adviser (\*)

## **IEA EBC Annex 58: Reliable Building energy performance characterisation based on full scale dynamic measurements**

### Annex 58 in general

To reduce the energy use of buildings and communities, many industrialised countries have imposed more and more stringent requirements in the last decades. In most cases, evaluation and labelling of the energy performance of buildings are carried out during the design phase. Several studies have shown, however, that the actual performance after construction may deviate significantly from this theoretically designed performance. As a result, there is growing interest in full scale testing of components and whole buildings to characterise their actual thermal performance and energy efficiency. This full scale testing approach is not only of interest to study building (component) performance under actual conditions, but is also a valuable and necessary tool to deduce simplified models for advanced components and systems to integrate them into building energy simulation models. The same is true to identify suitable models to describe the thermal dynamics of whole buildings including their energy systems, for example when optimising energy grids for building and communities.

It is clear that quantifying the actual performance of buildings, verifying calculation models and integrating new advanced energy solutions for nearly zero or positive energy buildings can only be effectively realised by in situ testing and dynamic data analysis. But, practice shows that the outcome of many on site activities can be questioned in terms of accuracy and reliability. Full scale testing requires a high quality approach during all stages of research, starting with the test environment, such as test cells or real buildings, accuracy of sensors and correct installation, data acquisition software, and so on. It is crucial that the experimental setup (for example the test layout or boundary conditions imposed during testing) is correctly designed, and produces reliable data. These outputs can then be used in dynamic data analysis based on advanced statistical methods to provide accurate characteristics for reliable final application. If the required quality is not achieved at any of the stages, the results become inconclusive or possibly even useless. The IEA EBC Annex 58-project arose from the need to develop the necessary knowledge, tools and networks to achieve reliable in situ dynamic testing and data analysis methods that can be used to characterise the actual energy performance of building components and whole buildings. As such, the outcome of the project is not only of interest for the building community, but is also valuable for policy and decision makers, as it provides opportunities to make the step from (stringent) requirements on paper towards actual energy performance assessment and quality checking. Furthermore, with the developed methodology it is possible to characterise the dynamic behaviour of buildings, which is a prerequisite for optimising smart energy and thermal grids. Finally, the project developed a dataset to validate numerical Building Energy Simulation programs.

### Structure of the project

Successful full scale dynamic testing requires quality over the whole process chain of full scale testing and dynamic data analysis: a good test infrastructure, a good experimental set-up, a reliable dynamic data analysis and appropriate use of the results. Therefore, the annex-project was organised around this process chain, and the following subtasks were defined:

**Subtask 1** made an inventory of full scale test facilities available all over the world and described the common methods with their advantages and drawbacks for analysing the obtained dynamic data. This subtask produced an overview of the current state of the art on full scale testing and dynamic data analysis and highlighted the necessary skills.

**Subtask 2** developed a roadmap on how to realise a good test environment and test set-up to measure the actual thermal performance of building components and whole buildings in situ. Since there are many different objectives when measuring the thermal performance of buildings or building components, the best way to treat this variety has

been identified as constructing a decision tree. With a clear idea of the test objective, the decision tree will give the information of a test procedure or a standard where this type of test is explained in detail.

**Subtask 3** focused on quality procedures for full scale dynamic data analysis and on how to characterise building components and whole buildings starting from full scale dynamic data sets. The report of subtask 3 provides a methodology for dynamic data analysis, taking into account the purpose of the in situ testing, the existence of prior physical knowledge, the available data and statistical tools,... The methodologies have been tested and validated within different common exercises, in a way that quality procedures and guidelines could be developed.

**Subtask 4** produced examples of the application of the developed concepts and showed the applicability and importance of full scale dynamic testing for different issues with respect to energy conservation in buildings and community systems, such as the verification of common BES-models, the characterisation of buildings based on in situ testing and smart meter readings and the application of dynamic building characterisation for optimising smart grids.

**Subtask 5** established a network of excellence on ‘in situ testing and dynamic data analysis’ for dissemination, knowledge exchange and guidelines on testing.

### Overview of the working meetings

The preparation and working phase of the project encompassed 8 working meetings:

Meeting	Place, date	Attended by
Kick off meeting	Leuven (BE), September 2011	45 participants
Second preparation meeting	Bilbao (SP), April 2012	46 participants
First working meeting	Leeds (UK), September 2012	44 participants
Second working meeting	Munich (GE), April 2013	53 participants
Third working meeting	Hong-Kong (CH), September 2013	26 participants
Fourth working meeting	Gent (BE), April 2014	49 participants
Fifth working meeting	Berkeley (USA), September 2014	37 participants
Sixth working meeting	Prague (CZ), April 2015	39 participants

During these meetings, working papers on different subjects related to full scale testing and data analysis were presented and discussed. Over the course of the Annex, a Round Robin experiment on characterising a test box was undertaken, and several common exercises on data analysis methods were introduced and solved.

### Outcome of the project

The IEA EBC Annex 58-project worked closely together with the Dynastee-network ([www.dynastee.info](http://www.dynastee.info)). Enhancing this network and promoting actual building performance characterization based on full scale measurements and the appropriate data analysis techniques via this network is one of the deliverables of the Annex-project. This network of excellence on full scale testing and dynamic data analysis organizes on a regular basis events such as international workshops, annual training,... and will be of help for organisations interested in full scale testing campaigns.

In addition to the network of excellence, the outcome of the Annex 58-project has been described in a set of reports, including:

Report of Subtask 1A: Inventory of full scale test facilities for evaluation of building energy performances.

Report of Subtask 1B: Overview of methods to analyse dynamic data

Report of Subtask 2: Logic and use of the decision tree for optimizing full scale dynamic testing.

Report of Subtask 3 part 1: Thermal performance characterization based on full scale testing: physical guidelines and description of the common exercises

Report of Subtask 3 part 2: Thermal performance characterization using time series data – statistical guidelines.

Report of Subtask 4A: Empirical validation of common building energy simulation models based on in situ dynamic data.

Report of Subtask 4B: Towards a characterization of buildings based on in situ testing and smart meter readings and potential for applications in smart grids

IEA EBC Annex 58 project summary report

## Participants

In total 49 institutes from 17 countries participated in Annex 58. The different participants are listed below:

Austria	Gabriel Rojas-Kopeinig, Universität Innsbruck Susanne Metzger, Vienna University of Technology
Belgium	Gilles Flamant, Belgian Building Research Institute Guillaume Lethé, Belgian Building Research Institute <b>Luk Vandaele, Belgian Building Research Institute (subtask 5 co-leader)</b> Paul Steskens, Belgian Building Research Institute Gabrielle Masy, Haute Ecole de la Province de Liège An-Heleen Deconinck, Katholieke Universiteit Leuven <b>Dirk Saelens, KU Leuven (subtask 4 co-leader)</b> <b>Geert Bauwens, KU Leuven (secretary)</b> Glenn Reynders, KU Leuven Ruben Baetens, KU Leuven Roel De Coninck, KU Leuven <b>Staf Roels, KU Leuven (operating agent)</b> Frédéric Delcuve, Knauf Insulation Philippe André, Université de Liège <b>Arnold Janssens, Universiteit Gent (subtask 1 leader)</b> Eline Himpe, Universiteit Gent
China	Gongshen Huang, City University of Hong Kong Tin-Tai Chow, City University of Hong Kong Linda Xiao Fu, The Hong Kong Polytechnic University <b>Shengwei Wang, The Hong Kong Polytechnic University (subtask 4 co-leader)</b> Xue Xue, The Hong Kong Polytechnic University
Czech Republic	Kamil Stanek, Czech Technical University Prague Pavel Kopecký, Czech Technical University Prague
Denmark	Christian Holm Christiansen, Danish Technological Institute Søren Østergaard Jensen, Danish Technological Institute <b>Henrik Madsen, Technical University of Denmark (subtask 3 co-leader)</b> Kyung Hun (Peter) Woo, Technical University of Denmark Peder Bacher, Technical University of Denmark
France	Bouchie Remi, Centre Scientifique et Technique du Bâtiment Pierre Boisson, Centre Scientifique et Technique du Bâtiment Mohamed El Mankibi, Ecole Nationale des Travaux Publics de l'Etat Christian Ghiaus, INSA de Lyon Ibán Naveros, INSA de Lyon Guillaume Pandraud, Isover Saint-Gobain Simon Rouchier, Université de Savoie
Germany	Franz Feldmeier, Fachhochschule Rosenheim Lucia Bauer, Fachhochschule Rosenheim Herbert Sinnesbichler, Fraunhofer-Institut für Bauphysik Ingo Heusler, Fraunhofer-Institut für Bauphysik Matthias Kersken, Fraunhofer-Institut für Bauphysik Soeren Peper, Passive House Institute
Italy	Fabio Moretti, ENEA <b>Hans Bloem, European Commission - DG JRC (subtask 5 co-leader)</b> Lorenzo Pagliano, Politecnico di Milano Giuseppina Alcamo, Università degli Studi di Firenze
The Netherlands	A.W.M. van Schijndel, Technische Universiteit Eindhoven Rick Kramer, Technische Universiteit Eindhoven
Norway	Nathalie Labonnote, Norges teknisk-naturvitenskapelige universitet
Spain	Gerard Mor-Lleida, Centro Internacional de Métodos Numéricos en Ingeniería Xavi Cipriano, Centro Internacional de Métodos Numéricos en Ingeniería <b>Aitor Erkoreka, Escuela Técnica Superior de Ingeniería Bilbao (subtask 2 co-leader)</b> Koldo Martin Escudero, Escuela Técnica Superior de Ingeniería Bilbao

Roberto Garay Martinez, Tecnalia Research & Innovation  
Luis Castillo López, CIEMAT  
**Maria José Jiménez Taboada, CIEMAT (subtask 3 co-leader)**  
Ricardo Enríquez Miranda, CIEMAT  
United Kingdom Richard Fritton, Salford University  
**Chris Gorse, Leeds Beckett University (subtask 2 co-leader)**  
Martin Fletcher, Leeds Beckett University  
Samuel Stamp, University College London  
Filippo Monari, University of Strathclyde  
United States **Paul A. Strachan, University of Strathclyde (subtask 4 co-leader)**  
Stephen Selkowitz, Lawrence Berkeley National Laboratory

# IEA, EBC Annex 58, Report of Subtask 1b

## Overview of methods to analyse dynamic data

Arnold Janssens

June 2016

### TABLE OF CONTENTS

- Symbols and units ..... 4
- 1. Introduction..... 5
- 2. Measurement of thermal transmittance of building components based on heat flux meters ..... 7
  - 2.1 Test procedure ..... 7
  - 2.2 Sources of errors..... 7
  - 2.3 Data analysis..... 8
    - 2.3.1 *Steady-state analysis* ..... 8
    - 2.3.2 *Dynamic analysis* ..... 9
  - 2.4 Application examples ..... 10
    - 2.4.1 *In situ measurement of the U-value of a very energy efficient building.* ..... 10
    - 2.4.2 *Opaque insulating panel.*..... 11
  - 2.5 References..... 12
- 3. Measurement of thermal and solar transmittance of building components tested in outdoor calorimetric test cells ..... 13
  - 3.1 Test procedure ..... 13
  - 3.2 Data analysis..... 14
    - 3.2.1 *Steady state analysis* ..... 14
    - 3.2.2 *Dynamic analysis* ..... 15
  - 3.3 Uncertainty analysis ..... 16
  - 3.4 Application examples ..... 16
    - 3.4.1 *Estimation of building component U-value tested in Mediterranean climate* .... 16
    - 3.4.2 *Analysis of building components tested in warm and sunny weather.*..... 17
  - 3.5 References..... 18
- 4. Measurement of heat transfer coefficient of whole buildings based on co-heating tests 19
  - 4.1 Test procedure ..... 19

4.2	Data analysis.....	20
4.2.1	<i>Steady state analysis</i> .....	20
4.2.2	<i>Disaggregation of heat loss components</i> .....	22
4.3	Recommendations for reliable results .....	23
4.3.1	<i>Testing period</i> .....	23
4.3.2	<i>Duration of the test</i> .....	23
4.3.3	<i>The determination of daily averaged data</i> .....	23
4.3.4	<i>Building type and form</i> .....	24
4.3.5	<i>Wind speed and direction</i> .....	24
4.4	References.....	24
5.	Rapid measurement of heat transfer coefficient of whole buildings based on transient heating .....	27
5.1	Test procedure.....	27
5.2	Data analysis.....	28
5.3	Recommendations for reliable results .....	30
5.4	Application examples .....	31
5.4.1	<i>Virtual buildings</i> .....	31
5.4.2	<i>Reference building: the Energy House at the University of Salford</i> .....	33
5.4.3	<i>Real buildings</i> .....	33
5.5	References.....	34
6.	Estimation of the energy signature of buildings in use based on energy use monitoring .....	35
6.1	Test procedure .....	35
6.2	Data analysis.....	35
6.2.1	<i>Relation between outdoor temperature and energy loss</i> .....	35
6.2.2	<i>Linear regression and Conditions of application</i> .....	36
6.2.3	<i>Robust regression of heating load curve based on q-q plot</i> .....	37
6.2.4	<i>Linear regression considering dynamic and solar gain effects</i> .....	38
6.3	Application example .....	38
6.4	References.....	39
7.	Grey box modelling of buildings in use based on dynamic energy use data.....	41
7.1	Data analysis method.....	41
7.1.1	<i>Model structure and parameter estimation method</i> .....	41
7.1.2	<i>Parameter estimation</i> .....	42
7.1.3	<i>Uncertainty estimation</i> .....	42
7.2	Model inputs and outputs .....	43
7.2.1	<i>Measurements</i> .....	43
7.2.2	<i>Output parameters</i> .....	44
7.2.3	<i>Advantages and drawbacks</i> .....	44

7.3	Application example .....	45
7.3.1	<i>Data</i> .....	45
7.3.2	<i>Two-state grey-box model of the heat dynamics of a building</i> .....	46
7.3.3	<i>Three-state grey-box model of the heat dynamics of a building</i> .....	48
7.3.4	<i>Parameter estimates</i> .....	51
7.4	Applications in literature .....	51
7.5	References.....	52

# Symbols and units

A	m <sup>2</sup>	Area
A <sub>sol</sub>	m <sup>2</sup>	Solar aperture
C	J/K	Effective heat capacity of a space or building
g	-	Total solar energy transmittance of a building element
H	W/K	Heat transfer coefficient of a building
H <sub>tr</sub>	W/K	Transmission heat transfer coefficient
H <sub>ve</sub>	W/K	Ventilation heat transfer coefficient (including infiltration)
I <sub>sol</sub>	W/m <sup>2</sup>	Solar irradiance
Q	J	Quantity of heat
q	W/m <sup>2</sup>	Heat flow density
R	m <sup>2</sup> K/W	Thermal resistance
T	K	Thermodynamic temperature
t	s	Time, period of time
U	W/m <sup>2</sup> K	Thermal transmittance
θ	°C	Centigrade temperature
Φ	W	Heat flow rate
Φ <sub>P</sub>	W	Thermal power

# 1. Introduction

A. Janssens (UGent)

The aim of the first subtask of IEA EBC Annex 58 was to give an overview and evaluation of previous and on-going in situ test activities based on a literature review and existing reports. An inventory was made of full scale test facilities for the evaluation of energy performances of building components and systems available at different institutes all over the world. Furthermore common methods were described to analyse the dynamic data obtained from full scale testing, with their advantages and drawbacks. The overview of full scale testing and dynamic data analysis is limited to energy performance characterization of either building components or whole buildings.

This report relates to the second part of the subtask, and gives an overview of existing data analysis methods, ranging from averaging and regression methods to dynamic approaches based on system identification techniques. These methods are discussed in relation to their application in following in situ measurements:

- measurement of thermal transmittance of building components based on heat flux meters;
- measurement of thermal and solar transmittance of building components tested in outdoor calorimetric test cells;
- measurement of heat transfer coefficient and solar aperture of whole buildings based on co-heating or transient heating tests;
- characterisation of the energy performance of whole buildings based on energy use monitoring.

Chapter 4 discusses the analysis of data obtained via the 'heat flow meter method', to define the in situ thermal transmittance of building components. Both steady-state and dynamic data analysis methods are presented to derive the thermal transmittance from the measured data.

Chapter 5 presents the methods used to analyse data obtained in outdoor calorimetric test cells. These test cells aim to obtain the thermal and solar characteristics of opaque or transparent building components under real dynamic outdoor conditions. As the overview shows, the emphasis has moved from steady state to dynamic methods with shorter test durations yielding improved information and more accurate results, with calculation of confidence intervals on the estimates in some cases.

Chapter 6 explains the analysis of measuring data of co-heating tests to estimate the heat transfer coefficient of a whole building. The focus of the chapter is on the use of linear regression techniques in relation with recommendations to set-up the experiment for reliable results.

Chapter 7 presents a specific test and analysis method, the QUB-method (Quick U-value of Buildings) as an example of a method developed to overcome the relatively long test duration of co-heating tests. These alternative test protocols, based on transient heating, take short-term data obtained in one or two days as a starting point to estimate the heat transfer coefficient of a building. To obtain reliable results a number of conditions have to be met.

Chapter 8 discusses linear regression methods, often referred to as energy signature techniques, applied to analyse energy monitoring data collected in buildings in use. This is done by investigating the correlation between the total energy consumption of the building over a given time step, and the corresponding climatic conditions. The chapter presents

solutions to extend energy signature techniques to the analysis of data on short time intervals, for instance obtained from energy monitoring systems.

Chapter 9 presents modelling techniques which describe the heat dynamics of the building to analyse high-time resolution energy monitoring data. An analysis technique that allows for energy performance characterisation without a detailed description of the building is grey-box modelling where prior physical knowledge is combined with data driven statistical modelling techniques. The parameters in the model are directly interpretable as representing the physical properties of the building, e.g. the heat transfer coefficient, effective heat capacities, or effective solar aperture.

Each chapter starts with a short description of the test procedure used to obtain measuring data, followed by the presentation of the data analysis method and uncertainty estimation, and a discussion of the advantages and drawbacks of the method. Finally each chapter concludes with some application examples and a list of references in literature. The chapters provide a general outline. Readers who are interested in a more detailed elaboration of the methods and applications presented in this book are referred to the references.

Throughout the different chapters the same symbols and terminology are used as proposed in the International Standard ISO 13790 on energy performance of buildings. However, since the figures in this book come from different sources, the legends and symbols used in the figures are not always consistent with ISO. If this is the case this is clarified in the figure caption or in the text.

## 2. Measurement of thermal transmittance of building components based on heat flux meters

G. Flamant (BBRI)

### 2.1 Test procedure

The in situ measurement of the thermal resistance and thermal transmittance is covered by the international standard ISO 9869 (1994) prepared by the Technical Committee ISO/TC163. This standard has been revised and republished in 2014 (ISO 2014). It describes the 'heat flow meter method' for the measurement of the thermal transmission properties of plane building components, primarily consisting of opaque layers perpendicular to the heat flow and having no significant lateral heat flow.

By the use of the 'heat flow meter method', the following thermal properties can be measured:

- The thermal resistance and thermal conductance, from surface to surface
- The total thermal resistance and transmittance, from environment to environment

The latter properties are more difficult to obtain because they require the knowledge of the 'environmental' temperatures at both sides of the component. The concept of the 'environmental' temperature combines the effects of heat transfer by convection and radiation at the outer and inner faces of the component. Due to changing weather and climatic conditions, the surface coefficients of heat transfer are not constant. Therefore it is preferable to determine the thermal properties from surface to surface instead of from environment to environment. In many cases it corresponds to what we are interested in.

The thermal resistance and thermal conductance of a plane element which is sufficiently homogeneous can be obtained by measuring :

- The density of heat flow rate through the component , by the use of a 'heat flow meter' typically mounted at the inner face of the component
- Surface temperatures at both faces of the component, by the use of thermocouples or flat resistance thermometers

Several sources of uncertainty exist and will be described in the next section. If a certain number of requirements are met, the revised draft of ISO/WD9869-1 indicates a total uncertainty between 14 % and 28 %.

### 2.2 Sources of errors

A list of the uncertainty/error sources is given below and is subdivided in 3 categories :

1. Error/uncertainty related the boundary conditions of the in situ measurement :
  - Imbalance of the heat flow rate
  - Edge heat loss
  - Accuracy in the position of each temperature sensor (on hot and cold side)
  - Non perfect contact between the heat flow meter and the inner face of the wall
  - ...
2. Error related to the measurement accuracy
  - Reading of the output of the heat flow meter
  - Reading of the temperature sensors

- Calibration of the heat flow meter
- Calibration of the temperature sensors
- 3. Error related to the analysis of data
  - Error caused by the analysis of non-steady state temperatures and heat flow rate

## 2.3 Data analysis

### 2.3.1 STEADY-STATE ANALYSIS

The average method assumes that the conductance or transmittance can be obtained by dividing the mean density of heat flow rate by the mean temperature difference. The average is calculated over a period of time long enough to reach convergence.

Eq. 4.1 gives the estimate of the average method of the surface to surface heat resistance after N measurements ( $R_N$  in [ $\text{m}^2\text{K/W}$ ])

$$R_{N,s-t0-s} = \frac{\sum_{k=1}^N (T_{i,s,k} - T_{o,s,k})}{\sum_{k=1}^N q_{i,s,k}} \quad (4.1)$$

This method is a straightforward analysis technique but shows drawbacks:

- The method yields no information on the dynamics of the component
- A long test duration is needed to obtain a relative accurate result
- The method ignores the possible effect of the short term variations in weather conditions on the properties of the component
- The method assumes that the heat content of the component is the same at the end and the beginning of the measurement period (same temperature and same moisture distribution)
- Uncertainties become too large when average heat flux density or temperature difference is small.

According to ISO (2014), the following conditions have to be fulfilled in order to carry out this method :

- The test duration has to exceed 72 hours (3 days).
- The estimate at the end of the test period should not deviate by more than 5% from the estimate at 24 hours before.
- The estimate corresponding to the first 2/3 part of the test period should not deviate by more than 5% from the estimate corresponding to the last 2/3 part of that period.
- During the experiment duration the wall should not be exposed to solar radiation and rain.
- The change in internal energy of the wall has to be less than 5% of the heat passing through the wall over the test period. One should estimate that change by the difference between the average temperature of the wall at the start of the test period and that temperature at the end of that period, multiplied by the specific heat and the wall's mass.

Some of these conditions are difficult to meet in practice when measuring the thermal performances of a completely unknown component. Nevertheless the application of this simple technique can be useful as a first step in the analysis process, providing some quantitative and qualitative information about the measured data.

The drawbacks mentioned above are mainly related to the measurement of medium to heavy elements. For (very) light building components (e.g. glazings), the steady-state analysis

performed on the data acquired at night (to avoid the effects of solar radiation) may deliver accurate results (see example in §4.4).

### 2.3.2 DYNAMIC ANALYSIS

The use of a dynamic method (identification method) has the big advantage to give information on the capacitance of the monitored component and shorten the test duration, particularly for medium to heavy elements submitted to variable indoor and outdoor temperatures (Bloem 1996).

The maximum time period between two records (temperatures and heat flux) and the minimum test duration depends on :

- the nature of the element (heavy, light, internal or external insulation);
- indoor and outdoor temperatures (average and fluctuations, before and during measurement);
- the method for analysis.

Several identification methods exist and can be applied for the determination of the in situ thermal resistance of components. Among these models, the use of lumped parameter model is convenient in many cases. This model is based on a series of RC-models representing the physical system: a wall is divided into different nodes that are interconnected with thermal conductances H and capacitances C.

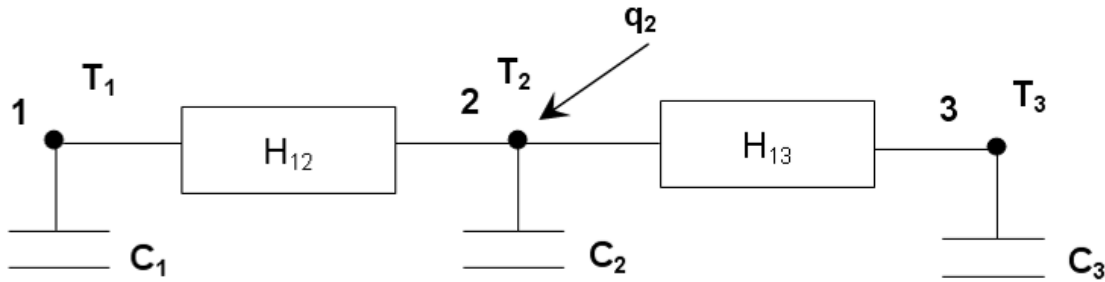


Figure 4.1: Heat balance on a single node 2.

Figure 4.1 shows an example. The heat balance at node 2 is observed:

$$C_2 \cdot \frac{dT_2}{dt} = (T_1 - T_2)H_{1-2} + (T_3 - T_2)H_{2-3} + q_2 \quad (4.2)$$

Where  $H_{1-2}$  and  $H_{2-3}$  are conductances and  $q_2$  an external heat flux that may be considered (solar radiation, heating or cooling system, etc.). An analogous differential equation is valid for every node with unknown temperature.

The model parameters comprise therefore the dynamic and steady state thermal properties of the system. The output of the actual test is then compared with the output which the model produces for the same conditions (input). The parameters are adjusted by iterations in order to reduce and minimise the deviation between measured and model output, the so-called objective function of which an example is presented in eq. 4.3. This iterative process is carried out with the aid of specialized software tools (e.g. LORD, CTSM). Figure 4.2 shows a scheme of the parameter identification principle.

$$V_N(\theta) = \frac{1}{N} \sum_{k=1}^N \varepsilon_k^2(\theta) = \frac{1}{N} \sum_{k=1}^N (T_{meas,k} - T_{calc,k})^2 \quad (4.3)$$

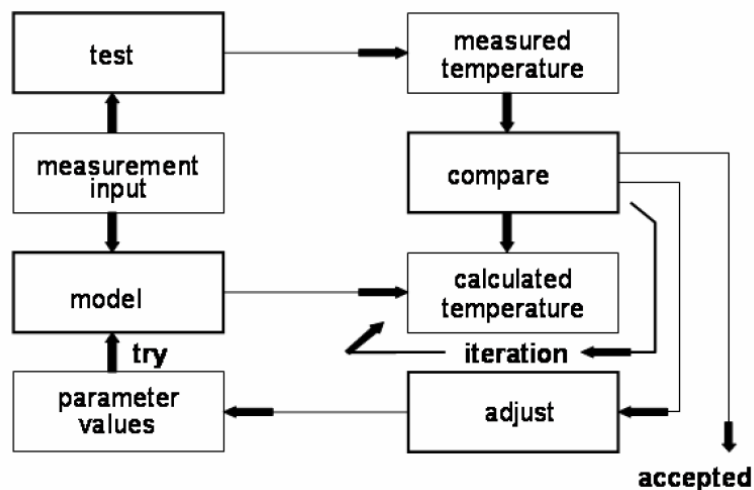


Figure 4.2: Principle of parameter identification.

It is needed to obtain statistical information on the reliability of the identified parameters. The reliability may be negatively affected by measurement and model errors and by correlation between parameters.

The main requirements for an appropriate model are as follows (Bloem 1994):

- The model should be able to accurately reproduce the steady-state and dynamic thermal processes.
- It should be able to relate the identified physical properties with definitions in international standards.
- It should not be too detailed, in the sense that it leads to 'over parameterisation', i.e. the situation in which some of the parameters cannot be identified because of strong correlation with other 'free' parameters in the model.
- It should preferably allow for prior knowledge to be used.
- It should preferably allow the option of adding specific non-linearities, such as a specific thermal resistance changing with temperature or with wind velocity, or solar transmittance changing with solar and sky conditions.

By adopting these requirements the model created should be 'transparent', i.e. a model in which the main elements of the heat balance of the tested component are recognised.

## 2.4 Application examples

### 2.4.1 IN SITU MEASUREMENT OF THE U-VALUE OF A VERY ENERGY EFFICIENT BUILDING.

A heat flow meter has been installed on the inner face of a triple glazing together with a thermocouple at the inner and outer faces, in order to check in situ the U-value declared by the manufacturer. The same procedure has been applied to measure the U-value of an opaque concrete wall insulated by an external thick insulating material (ETIC system). Both glazing and opaque wall are oriented to the north.

Figure 4.3 gives the measured 'average' heat flux in function of the 'average' temperature difference between inside and outside (in this case, 'average' means average of the 5 minutes data during 4 hours). For the glazing, only hours during night time have been considered.

One can clearly see a good linear regression between heat flux and temperature difference in the case of the glazing; the application of the average method gives results with good accuracy. On the other hand, the average method is not appropriate for the thick insulated

wall due to the high insulation level and high thermal mass. In this latter case, a longer averaging time of at least 72 hours is required, or a dynamic method may provide reliable results.

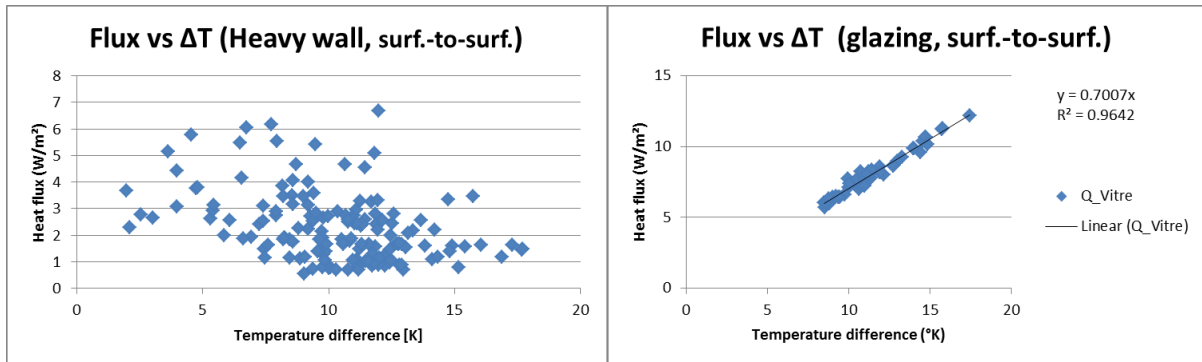


Figure 4.3: Linear regression between heat flux and temperature difference. Left: heavy wall with thermal insulation; right: triple glazing unit.

#### 2.4.2 OPAQUE INSULATING PANEL

This section discusses results of a measuring campaign where the thermal performance of an insulating panel with thickness 20 cm is determined. The insulating material is protected by inner and outer wood sheets. Therefore this panel is characterised by a high thermal resistance but by a low thermal mass. Before using dynamic methods, some steady-state calculations have been done as a first step to estimate the U-value.

The average method has been applied by increasing the length of observations with a timestep of 1 day. Figure 4.4 shows the average surface-to-surface conductance versus the number of days. By averaging the data on the whole test period (8 days), the steady state calculation gives a U-value of 0.183 W/m²K.

As mentioned above, the average method can deliver results with reasonable accuracy for walls with low thermal mass but requires duration of minimum 6 to 8 days (in this case) to reach convergence.

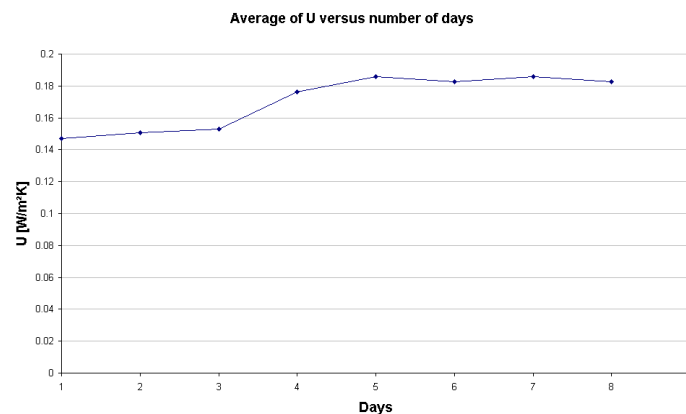


Figure 4.4: Result of average method as a function of number of days of analysis

Also a dynamic method has been applied. Figure 4.5 shows the model chosen for identification of the one-dimensional surface-to-surface conductance: a thermal network of 2 capacitances and 3 conductances. Experience has shown that this model is appropriate for this kind of component.

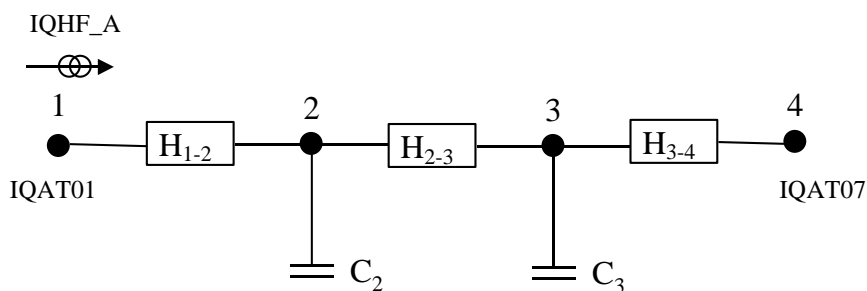


Figure 4.5: Model for identification of the conductance of the opaque component

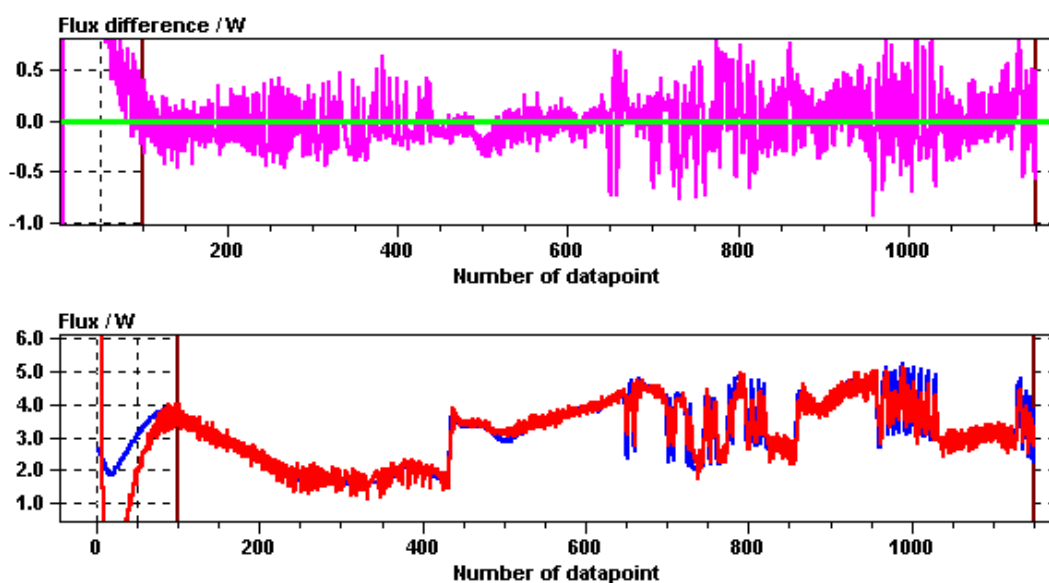


Figure 4.6: Identification results for output variable IQHF\_A

The input variables are the internal surface temperature IQAT01 and the external surface temperature IQAT07. Heat flux IQHF\_A has been used as output. The surface to surface one-dimensional conductance of the component is calculated as the steady state heat flow between the nodes IQAT01 (inside surface temperature) and IQAT07 (outside surface temperature) for 1K temperature difference between these two points. The identification gives a surface-to-surface U-value of **0.179 W/m<sup>2</sup>K ± 0.4%**, which is very close to the value determined by the average method. The residue is distributed randomly around zero, as Figure 4.6 demonstrates.

## 2.5 References

1. Bloem J.J. (ed.) 1994, System Identification Applied to Building Performance Data, EUR 15885 EN
2. Bloem J.J. (ed.), 1996, System Identification Competition, ISBN 92-827-6348-X, EUR 16359 EN
3. ISO 9869, Thermal insulation – building elements – In situ measurements of thermal resistance and thermal transmittance , 1994
4. ISO/WD 9869-1, Thermal insulation – building elements – In situ measurements of thermal resistance and thermal transmittance – Part 1 : heat flow meter method, 2014

### 3. Measurement of thermal and solar transmittance of building components tested in outdoor calorimetric test cells

G. Alcamo (DIDA), A. Erkoreka (UPV/EHU), M.J. Jiménez (CIEMAT)

#### 3.1 Test procedure

Calorimetric test cells aim to obtain the thermal and solar characteristics of building components under real dynamic outdoor conditions. In general, neither the heat loss, nor the solar heat gain through the component, can be measured directly because of the simultaneous occurrence of a variety of heat transfer mechanisms through the component. However, these quantities can be inferred indirectly based on the measurement of the net heat flow through the building component. Calorimetric test cells are specifically designed to measure this latter quantity in an accurate way. Since the net heat flow through the component is related to its thermal and solar characteristics, the measurement of the time-series of the net heat flow and of internal and ambient conditions (temperature, global solar radiation perpendicular to component, wind speed,...) allows to identify these performances. The idea of measuring the heat flow rate through a building component in an indirect way is crucial when non-homogeneous or (semi-)transparent samples are tested where the heat flux meter method is not applicable.

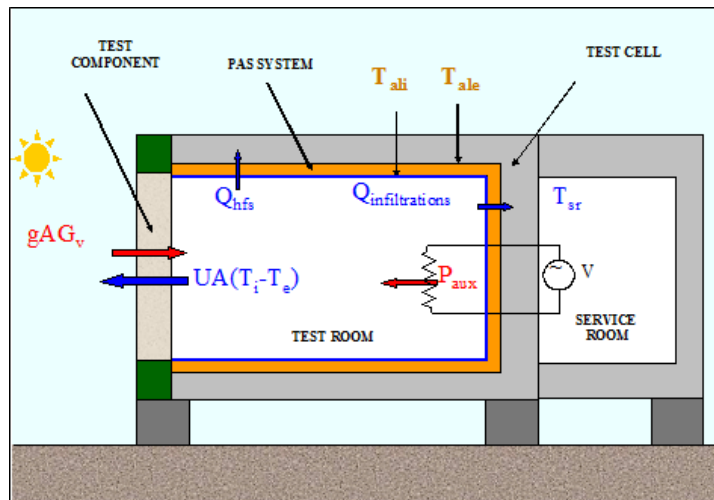


Figure 5.1: Schematic view of the heat balance in the PASLINK test cell (Jimenez et al. 2008)

Figure 5.1 shows a cross section through a typical test cell as an example: the well-known PASLINK cell. The measuring principle is explained here by means of the steady-state heat balance of the test room:

$$\Phi_{net,c} = P_{aux} - \Phi_{tc} - \Phi_{sr} \quad (5.1)$$

where  $\Phi_{net,c}$  is the net heat flow rate (W) from the test room through the component to the exterior (to be defined);  $P_{aux}$  is the heating power (W) supplied to the test room (measured, allowing for any cooling extraction);  $\Phi_{tc}$  is the heat flow rate (W) from the test cell to the

exterior across the test room envelope (measurement method depends on the type of test cell);  $\Phi_{sr}$  is the heat flow rate (W) from the test cell to the service room across the partition wall (measurement method depends on the type of test cell).

To define the component's characteristics, the net heat flow rate is expressed in terms of its heat loss and heat gain parts, for example in steady state conditions:

$$\Phi_{net,c} = H(T_i - T_e) - A_{sol}I_{sol,v} \quad (5.2)$$

Where H is the heat transfer coefficient (W/K) of the component (in the figures the notation UA is used);  $T_i$  and  $T_e$  are the measured internal and external temperatures respectively (K),  $A_{sol}$  is the solar aperture (m<sup>2</sup>) of the component (in the figures the notation gA is used);  $I_{sol,v}$  is the measured solar irradiance (W/m<sup>2</sup>) in the plane of the component.

The accuracy of the test cell largely depends on the measuring method used to determine the heat flow rate through the envelope of the test cell (the last two terms in eq. 5.1), and on the response of the HVAC system used to supply or extract heat to the test room.

In early test cells, like the ones that were developed in the PASSYS-project starting in 1985, the heat flow rate through the envelope of the test cell was obtained from prior calibration measurements and from measurement of temperatures at the internal and external surface of the test room envelope during the actual test. This methodology however required too long testing periods and the test results were limited to some steady state characteristics of the tested sample.

Two methods for allowing a more accurate measurement of the heat flow rate through the envelope of the test room were developed by the PASLINK network inside the COMPASS European project. The Pseudo Adiabatic Shell (PAS) consists of an electric heating foil used to compensate for the heat loss through the test room envelope. Fig. 5.1 shows a vertical section of the test cell with the PAS installed. The mean temperature difference between the aluminium plates at both sides of the PAS is measured by thermopiles. The thermopile signal is used to control the heating foil in such a way that the resulting heat flux comes close to zero. On the other hand, the idea of TNO (Building and Construction Research, Delft, Netherlands) was to substitute the PAS by custom made heat flux sensors in the form of tiles covering all the internal surfaces of the test room. The advantage is that the thickness of the elements is only a few millimetres and that direct measurements of rapid changes may be possible thanks to the fast thermal response of the tiles. These concepts are further improved in more recent test cell designs, eg in the University of Florence the use of heat flux tiles with integrated Peltier cells was investigated, and at Fraunhofer a PAS-like concept was implemented by means of water-bearing absorbers (Janssens 2016).

By means of the two previous methods, higher accuracy is obtained and the duration of the test sequence can be reduced significantly. Within 1 week of measurements sufficient information is gained to determine the main thermal parameters. This is an important cost reduction.

## 3.2 Data analysis

### 3.2.1 STEADY STATE ANALYSIS

Based on the steady-state heat balance of the test room, successive averaged measurements under different boundary conditions allow to derive the components steady-state characteristics. The analysis is based on the rearranged form of equation 5.2:

$$\frac{\Phi_{net,c}}{T_i - T_e} = H - A_{sol} \frac{I_{sol,v}}{T_i - T_e} \quad (5.3)$$

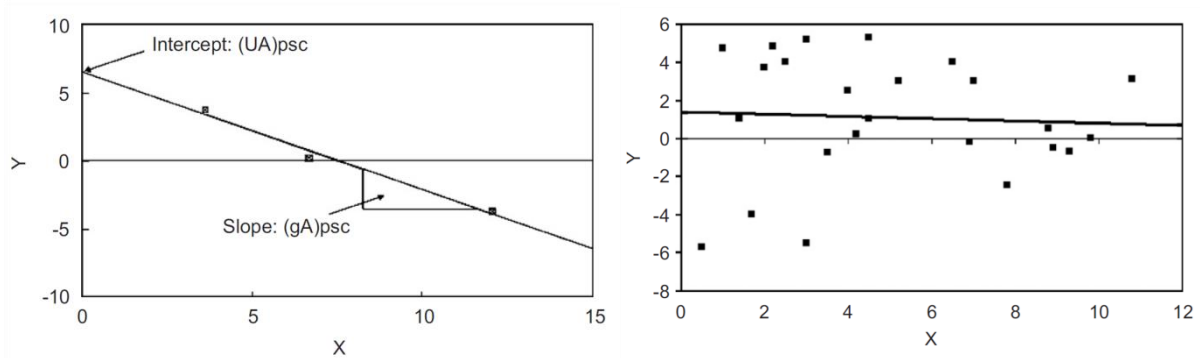


Figure 5.2: illustration of a steady-state regression analysis using different integration periods: 10 day mean values (left), 1 day mean values (right) (Baker and van Dijk 2008). The symbols UA and gA in the figure correspond to H and  $A_{sol}$  in Eq. 5.3.

A graphical (X,Y) plot, with  $Y = \Phi_{net,c}/(T_i-T_e)$  and  $X = I_{sol,w}/(T_i-T_e)$ , gives a linear relationship for which in principle only two distinct measurement points are needed to yield the performance characteristics of the components. With more points the H- and  $A_{sol}$ -values are obtained by linear regression analysis, as illustrated in Fig. 5.2. While the steady state method is a straightforward, simple measurement technique, it has significant disadvantages, comparable to the drawbacks mentioned in § 4.3.1 for the heat flow meter method:

- The test duration should be sufficiently long to average out the influence of dynamic effects and obtain accurate results.
- The method yields no information on the dynamics of the system e.g. thermal capacitance, time constants, etc.
- Given the inertia of the test cell and of some highly insulated and/or heavy mass building components, an integration period of more than a week may be required, as illustrated in Fig. 5.2. When the integration period per point in the graph is only 24 h instead of 10 days, the daily average heat loss through the component is strongly influenced by the history of the previous days. The illustrated linear regression line does not provide meaningful information in this case.

In some works a first order correction is mentioned, as an alternative to solve some of the problems related to the application of linear regression method based on averages to dynamic tests of building components, leading to pseudo-dynamic models using daily averages, although dynamic methods are pointed out as more appropriate for such applications (Van Dijk and van der Linden 1993, Bloem and Martin 2001).

### 3.2.2 DYNAMIC ANALYSIS

In order to overcome the disadvantages of the steady state analysis methods, the emphasis has moved from steady state to dynamic methods with shorter test durations yielding improved information and more accurate results, with calculation of confidence intervals on the estimates in some cases. These methods are based on dynamic energy balance equations of the considered physical systems and the application of system identification techniques to obtain the parameters of interest. In parallel with improvements in test methodology as described above, software tools have been developed to enable the identification of the component characteristics and provide statistical information on the identified parameters.

Different modelling approaches are used in system identification of building components (Jiménez and Madsen 2008). A lumped parameter RC model written as finite differences formed the basis for the LORD software (Gutschker 2008). Whilst LORD has been tailored to the specific requirements of the PASLINK Network, e.g. test cell experiments, it can easily be used for the analysis of other thermal systems. Continuous time linear stochastic modelling

(CTLSM) is a stochastic method that takes into account uncertainties in both the measurements and calculations. CTLSM is a semi-physical modelling approach using state-space models described by stochastic differential equations and has evolved into the continuous time stochastic modelling (CTSM) software (Kristensen and Madsen 2003). CTSM has been used for estimating and identifying physical systems and performances, such as the heat dynamics of an entire building, the thermal characteristics of walls, the dynamics of heat exchangers, radiators and thermostats, etc. An important issue on dynamic data analysis is the experience of the user since for the same data series, same software and same parameters to be identified, different results may be obtained depending on the user.

Another issue that must be addressed in data analysis is the correct assignment of inputs and outputs, once the energy balance equations are defined. This decision must be based on physical criteria such as causality and correlations between measured variables. Sometimes this assignment is evident and a single output approach is enough to afford the analysis. Sometimes tests can be set up to enhance this single output approach, for example using ROLBS or PRBS power sequences that excite the system and de-correlate variables. However in some circumstances the usefulness of these sequences is very limited. This is the case when temperature difference between indoors and outdoors is low, high solar radiation is present, and when the building envelope is highly insulated. Under these circumstances the amplitude of the heating sequence is drastically limited, and consequently, it is less effective as a test strategy, which makes identification of the required parameters more difficult. This problem is very frequent, even in winter, in locations with warm and sunny weather such as the south of Spain. An alternative to overcome these problems is using multi-output models. A case study successfully applying this approach is summarised by Jiménez and Heras (2005).

### **3.3 Uncertainty analysis**

In commercial tests of building components carried out by CIEMAT, uncertainty is estimated according to the “ISO Guide to the expression of uncertainty in measurement” (ISO 1995). The applied procedure adapted to estimate the uncertainty of the thermal parameters identified from dynamic tests is described in detail by Jiménez (2005) and summarised in a PASLINK report (2003).

One of the key steps in the applied procedure is the estimation of each sensitivity coefficient as specified by the ISO guide. Taking into account that the characteristic parameters are obtained numerically from time series of measurements, and it is not practical to establish an analytical expression of these parameters as function of every measurement used to estimate its value, the estimation of each sensitivity coefficient  $c_i$  corresponding to variable  $x_i$ , as the corresponding partial derivative becomes almost impossible. The adopted option as suggested in the ISO guide for these cases, is to obtain the product  $c_i u(x_i)$ , calculated as half of the difference of the changes in the parameter estimate, due to changes in the input estimate equal to its uncertainty  $u(x_i)$  and  $-u(x_i)$ . The final estimation includes a coverage factor  $K=2$  that was applied for a 95% confidence interval, as recommended by the ISO guide.

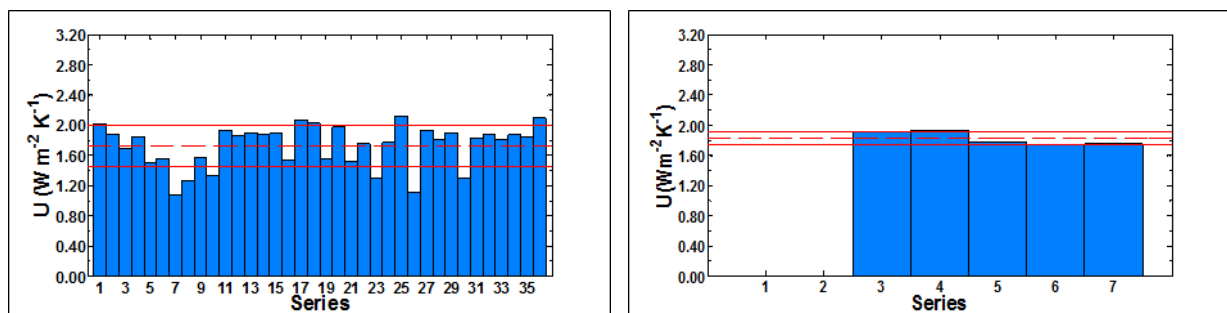
### **3.4 Application examples**

#### **3.4.1 ESTIMATION OF BUILDING COMPONENT U-VALUE TESTED IN MEDITERRANEAN CLIMATE**

The work by Naveros et al. (2012) investigates the capabilities and limitations of the average and linear regression methods applied to the thermal performance analysis of real size

building components tested in dynamic outdoor weather conditions, considering the analysis to obtain the air to air U value of a homogeneous opaque wall tested in the South East of Spain.

This study aims to distinguish which of the problems observed in these methods are specifically related to the regression average method such as the minimum integration period, and which are related to general aspects such as the minimum terms necessary in the energy balance equation which should also be solved in dynamic approaches. Integration periods from one to ten days have been considered. A noticeable improvement was observed as the integration period was increased from one to five days. Larger integration periods did not show significant improvements. The influence on the energy balance equation of global solar radiation, longwave radiation and wind speed has been analysed.



(a) Using 1 day averages and linear regression including  $T_i-T_e$ ,  $I_{sol,v}$  and without y-intercept. Results for different data sets present a large variation that cannot be explained.

(b) Using 5 days averages and linear regression including  $T_i-T_e$ ,  $I_{sol,v}$ , wind speed, and y-intercept. (U not available for series 1 and 2 because wind speed not available). Improvement in agreement of results for different series.

Figure 5.3: Data analysis of a homogeneous opaque wall using linear regression methods

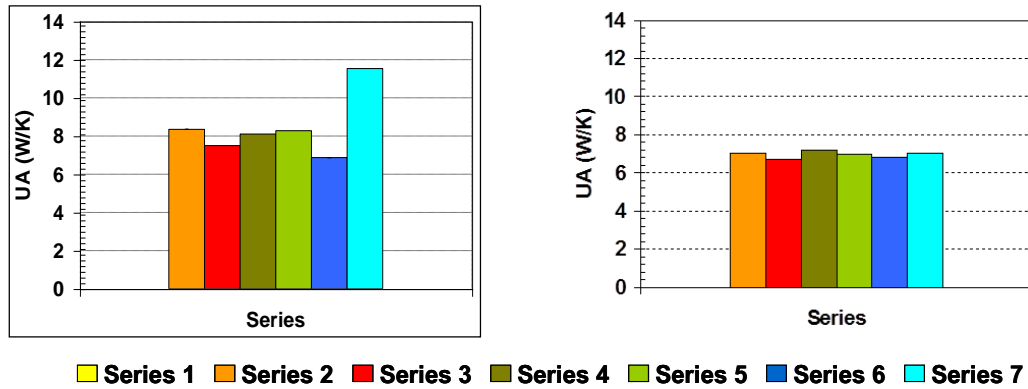
Significant improvements have been observed when including wind speed. Although it was possible to obtain accurate results, the main drawback of this method is that an excessively long test period is required to obtain reliable parameter estimates. Examples of results are presented in Figure 5.3.

### 3.4.2 ANALYSIS OF BUILDING COMPONENTS TESTED IN WARM AND SUNNY WEATHER

An experiment carried out by CIEMAT in Almería, south east of Spain shows the application of non-linear models when testing and analysing a wall with window component using test cells in warm sunny weather (Jimenez et al. 2008).

Several linear models were used at test-cell level. First, traditional RC linear models, then a wider and more general set of linear transfer function models (ARX), and more detailed state space model were progressively developed.

When the most commonly used RC models and more general linear transfer function models were used to estimate UA and gA, the analyses showed wide discrepancies between the results and their expected values, as well as between the results obtained for different datasets. Remarkably better and realistic estimates of UA and gA were achieved in the test-cell-level analysis when the effect of the long wave exchange in the indoor surface of the test cell was considered as a non-linear boundary effect. This improvement is noticeable when the non-linear effect is approximated using transfer function models, but it is emphasized even more by considering a slight difference between the air temperature in the test room and the temperature of the corresponding sensor in a more detailed non-linear state space model. Examples of results are presented in Figure 5.4.



(a) Estimates using RC linear models with traditional assumptions leading to physically unrealistic results.

(b) Estimates using state-space model considering the longwave heat exchange at inner surfaces of the test cell, leading to consistent results.

Figure 5.4: Window tested in a test cell. Test conditions in series 1 to 5 in summer, 6 and 7 in winter. 2 to 6 with test cell facing north. 1 and 7 with test cell facing south.

### 3.5 References

1. Bloem, J.J., and S. Martin. 2001. A pseudo dynamic analysis tool for thermal certification of dwellings. *Energy and Buildings*. 33, pp. 207-212.
2. Gutschker, O. 2008. Parameter identification with the software package LORD. Special issue on Outdoor testing, analysis and modelling of building components. *Building and Environment*. 43(2), pp. 163-169.
3. International Standardisation Organization. ISO Guide to the expression of uncertainty in measurement. Ginebra, 1995. ISBN 92-67-10188-9.
4. Inventory of full scale test facilities for evaluation of building energy performances (A. Janssens, ed.). 2016. IEA EBC Annex 58, Subtask 1, Final report.
5. Jiménez, M.J., M.R. Heras. 2005. Application of multi-output ARX models to estimate the U and g values of building components from outdoors testing. *Solar Energy*. 79(3), pp. 302-310.
6. Jiménez, M.J. 2005. In Spanish. "Caracterización de cerramientos constructivos mediante células de ensayo de Intemperie. Aplicación del cálculo de incertidumbres a la optimización de los ensayos". Ph. D Thesis carried out at CIEMAT and presented at Almería University.
7. Jiménez, M.J., H. Madsen. 2008. Models for Describing the Thermal Characteristics of Building Components. *Building and Environment*. Special issue on Outdoor testing, analysis and modelling of building components. 43(2), pp. 152-162.
8. Jiménez, M.J., B. Porcar, M.R. Heras. 2008. Estimation of UA and gA values of building components from outdoor tests in warm and moderate weather conditions. *Solar Energy*. 82(7), pp. 573-587.
9. Kristensen, N.R., H. Madsen. 2003. Continuous Time Stochastic Modelling - CTSM 2.3 User Guide. Technical University of Denmark, Lyngby, Denmark.
10. Naveros, I., M.J. Jiménez, M.R. Heras. 2012. Analysis of capabilities and limitations of the regression method based in averages, applied to the estimation of the U value of building component tested in Mediterranean weather. *Energy and buildings*. 55. pp. 854-872.
11. PASLINK-EEIG. IQ-Test final technical report. IQ-TEST project, CONTRACT N°: ERK6-CT1999-20003, PROJECT N°: NNE5-1999-0511. 1<sup>st</sup> August 2003.
12. van Dijk, H.A.L., G.P van der Linden. 1993. The PASSYS Method for Testing Passive Solar Components. *Building and Environment*. 28 (2), pp. 115-126.

## 4. Measurement of heat transfer coefficient of whole buildings based on co-heating tests

G. Bauwens (KU Leuven), S. Stamp (UCL), D. Johnston (Leeds Beckett)

### 4.1 Test procedure

A common method to evaluate the thermal performance of a building in situ is the co-heating test. It represents a quasi-stationary method based on linear regression analysis of dynamic measurement data.

With a co-heating test the total heat transfer coefficient (combined transmission and ventilation heat loss), denoted  $H$ , in  $W/K$  and the solar aperture in  $m^2$  of an unoccupied dwelling are estimated. The heat transfer coefficient incorporates losses through all mechanisms and across the entire building envelope and includes variations in the fabric and through unpredicted thermal processes.

The co-heating method works by using an approximated or quasi-steady state energy balance. During the test, an unoccupied dwelling is homogeneously heated to an elevated steady-state interior temperature (e.g.  $25^{\circ}C$ ), using electric resistance point heaters, thermostatic controllers and ventilators. The internal heat gains from these devices are measured directly via kilowatt-hour meters, a quantity defined as electric power. Additionally, the indoor and outdoor temperatures, wind speed and direction, and solar radiation are monitored throughout the test.

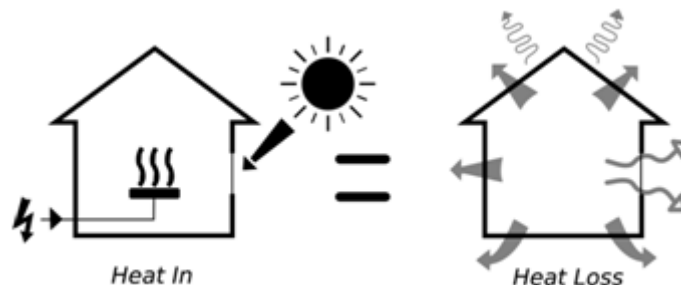


*Figure 6.1: Co-heating principal. At constant internal temperature, the heat input (from electric heaters and solar gains) is equal to the total heat loss across the building envelope.*

Hence, the co-heating test essentially consists of a thermostatic heating procedure stretched over a longer period of time. The effect of charging and discharging the thermal mass of the building is thereby diminished. As a basis for analysis, the measurement data is averaged over a significant time-span (1 day, 2 days, week, ...). Both factors serve to explain the quasi-stationary nature of the co-heating test methodology. The term quasi refers to the varying external weather conditions, which impedes the test from being truly steady-state. The co-heating method arose from work at a number of locations in the late 1970s and early 1980s including at the US Solar Energy Research Institute (Sonderregger, 1979; Balcombe, 1992), and at ECRC in the UK (Siviour 1981). The method was explored and developed by Subbarao et al., (1988) and Everett (1985). In the UK, sporadic use of the method through the 1990s was followed by an intense period of activity at Leeds Metropolitan University, which resulted in the development of the current UK experimental guidelines (Wingfield et al., 2010, Johnston et al. 2013).

The co-heating test itself is often combined with further testing methods and a forensic examination of the building. As an example, elevated and stable internal temperatures can assist a thermography survey, with particularly good results observed during a depressurisation test at the end of the co-heating test. Additionally, heat flux sensors, temperature traces and partial deconstruction of the fabric can all help researchers determine more about a building's thermal performance, with more accuracy.

In order to undertake a successful co-heating measurement campaign, tailored equipment is indispensable. A number of electric heaters and ventilators serve to heat up the dwelling to an elevated, uniform and constant indoor air temperature. The obtained indoor air temperatures and relative humidities are monitored. Additionally, the outdoor air temperature, relative humidity, solar radiation, wind speed and direction and rainfall are monitored at a weather station placed close to the investigated dwelling. All sensor data is transmitted to a centrally placed logger.

## 4.2 Data analysis

### 4.2.1 STEADY STATE ANALYSIS

The co-heating test essentially assumes the following stationary heat balance on the investigated building (based on Everett, 1985):

$$\Phi_P + \sum A_{sol} I_{sol} = H \cdot (T_i - T_e) = H \cdot \Delta T \quad (6.1)$$

where  $\Phi_P$  is the energy supplied by heaters and dissipated by ventilators [W];  $I_{sol}$  is measured or calculated solar irradiance [ $W/m^2$ ];  $T_i - T_e = \Delta T$  is the temperature difference inside-outside. As the estimated heat transfer coefficients depends largely on the established  $\Delta T$  it is important that representative internal and external temperatures are used. A representative  $T_i$  needs to be constructed from the measured indoor air temperatures in the different zones of the dwelling: by (1) plain averaging, (2) weighting by volume or surface, (3) weighting by assumed associated heat loss of respective zones, (4) applying principal component analysis. Weighting can be useful in instances where zones associated with sensors are extreme in size or heat loss, i.e. large-small volumes and/or low-high heat loss elements. In general, however dependent on the quality of the experiment ( $T_i$  is thermostatically controlled in most dwelling zones), the choice of weighting method can be expected to be of little importance.

The solar aperture  $A_{sol}$  [ $m^2$ ] and the overall heat transfer coefficient  $H$  [W/K] express the relation between  $\Phi_P$  as a dependent variable and  $I_{sol}$  and  $\Delta T$  as independent variables.  $A_{sol}$  can be read as a global solar aperture per orientation which comprises the influence of non-perpendicular incidence of solar radiation, geometry (including possible shading) and orientation of the building, solar absorption at opaque surfaces, solar energy transmittance factor and glazing surface of the building envelope. Essentially, it relates the effective internal solar heat gains to the externally measured solar radiation.  $A_{sol}$  can be derived experimentally from the co-heating data or estimated from properties of the buildings and its glazing (e.g. SAP, 2009), although calculation methods rely on many assumptions and typically ignore gains through opaque elements. Solar heat gains will also have an effect on the amount of heat that is lost through non-habitable areas of the dwelling that are outside the buildings thermal envelope. Such areas include cold ventilated roof spaces and knee walls.

The analysis of co-heating measurement data (time averaged data points for  $\Phi_P$ ,  $I_{sol}$  and  $\Delta T$ ) is commonly done using linear regression techniques. The advantage over plain averaging is that possible outliers can be taken into account in a more sensible way. Often data will need to be removed from the beginning of the test, whilst the dwelling is being heated up and the thermal mass charged. A simple average of total power input and average temperature

difference across the valid test period can be useful as a check on the regression process itself, particularly when there is not a wide spread in data points.

Assuming the heat balance in Equation 6.1 to hold, the parameters of interest, are generally determined by applying simple or multiple linear regression techniques on co-heating measurement data (c being a constant heat loss term, see Bauwens and Roels 2014):

$$\Phi_P + A_{sol}I_{sol} = H \cdot \Delta T + c \quad (6.2)$$

Essentially, three options can be discerned:

1. The energy supplied to the interior under the form of electrical energy can, e.g. on a daily average basis, be corrected for solar gains and plotted as a function of  $\Delta T$  (Fig. 6.2(a), where the notation HLC, heat loss coefficient, is used for the heat transfer coefficient H). This correction implies that the solar aperture parameter  $A_{sol}$  is calculated. Information of factors such as the total glazing area, the orientation of the glazing, the glazing solar transmittance, the solar access factor, the frame factor and the average incidence factor can serve as input here. Once calculated, the solar aperture is multiplied with the measured averaged solar radiation, to calculate the averaged solar gains  $A_{sol}I_{sol}$ . These values then serve to correct the raw heat input to the dwelling.
2. An alternative to the method described above is to, aside from  $\Delta T$ , consider  $I_{sol}$  as an additional independent variable explaining the variability of  $\Phi_P$ . Multiple regression techniques allow to determine both H and  $A_{sol}$  in Eq. 6.2 (Lowe et al., 2007, Everett, 1985).
3. A third method is based on dividing all terms in Eq. 6.2 by  $\Delta T$ . By doing so, an equation is attained on which a simple linear regression can be performed, assuming  $\Phi_P/\Delta T$  as dependent variable and  $I_{sol}/\Delta T$  as independent or explanatory variable, as in Eq. 6.3.

$$\frac{\Phi_P}{\Delta T} = H - A_{sol} \frac{I_{sol}}{\Delta T} \quad (6.3)$$

As illustrated in Figure 6.2(b), an estimate of H is then given by the intercept. An advantage of this method is that the solar aperture can also be read as the slope of the regression line. In the figure the notation HLC is used for the heat transfer coefficient H and  $A_{sw}$  for the solar aperture  $A_{sol}$ . Note that this mathematical transformation implicitly forces the above described multiple linear regression through zero. In both of the earlier mentioned cases, a non-zero intercept is possible due to discrepancies between the measurement data and the assumed stationary model to which it is fitted.

All of the options described above result in estimates for the heat transfer coefficient. The second and third methods additionally lead to estimations of the solar aperture. Although the solar aperture has lost much of its physical meaning in the analysis, it is important to quantify this parameter in those cases where solar radiation is significant during the experiment. In order for the solar radiation  $I_{sol}$  to be of significant influence on the necessary heating power  $\Phi_P$ , i.e. in order to have sufficient confidence  $A_{sol}$  differs from zero, a sufficient spread in solar radiation needs to be observed during the test. None of the options consider other factors that in some cases have a significant influence on the heat input into the dwelling, such as wind speed, wind direction and fabric moisture levels.

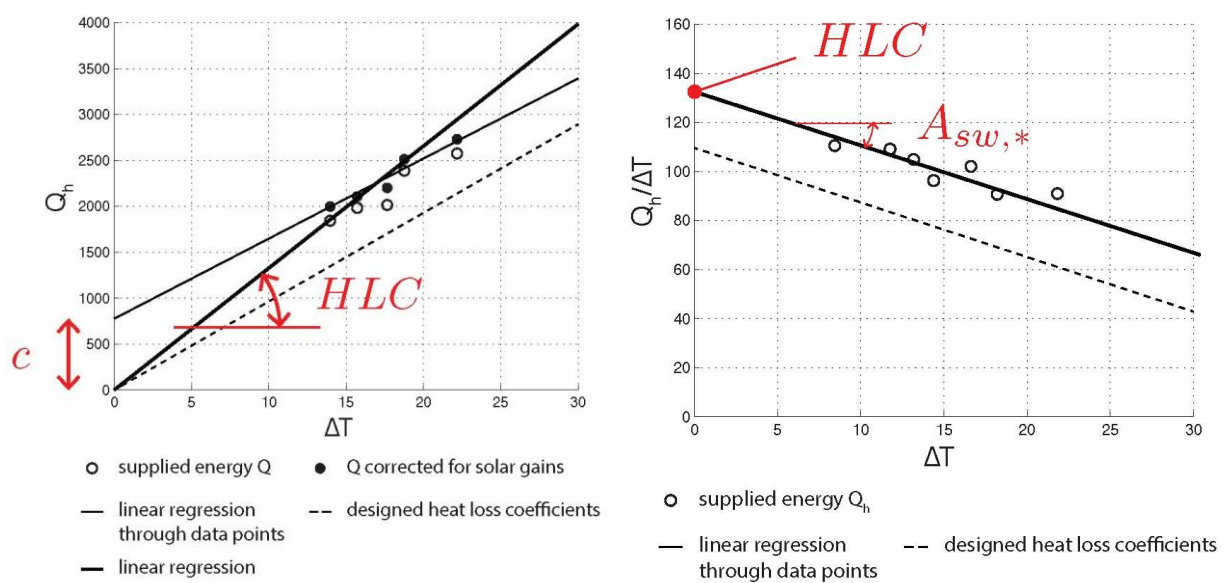


Figure 6.2: Estimation of heat transfer coefficient and solar aperture by applying simple linear regression – a (left): based on eq. 6.2; b (right): based on eq. 6.3 (Bauwens 2014).

#### 4.2.2 DISAGGREGATION OF HEAT LOSS COMPONENTS

The amount of heat loss that is measured during a co-heating test comprises two main components: fabric heat loss  $H_{tr}$  and background ventilation heat loss  $H_{ve}$ . The proportional split between these two components can be estimated if the magnitude of one of the components is known.

In the case of the background ventilation heat loss, it is possible to undertake various measurements during the test in order to determine the background ventilation rate. The background ventilation rate can then be used to calculate the background ventilation heat loss during the test. Three separate approaches can be adopted to determine the background ventilation rate (Liddament M. 1996). These are as follows:

1. Fan pressurization technique;
2. Tracer gas decay method;
3. Constant concentration tracer gas method

The fan pressurization technique involves undertaking a pressurization test immediately before the commencement of the co-heating test and immediately after the end of the co-heating test. The average of the two measurements is then used to give a reasonable approximation of the average air leakage rate achieved within the building over the period of the co-heating test.

The background ventilation rate  $n_{inf}$  can then be approximated using the simple  $n_{50}/20$  rule of thumb. This involves dividing the air leakage rate in air changes per hour at 50 Pa by 20. A correction factor can then be applied to the figure to take account of the leakage exponent, the building geometry, the height of the dwelling and any sheltering from neighbouring buildings. Suitable values for the correction factor are normally given in the national calculation methodologies for the energy performance of buildings.

It is important to realize that inherent within the above procedure is the assumption that ventilation heat loss has a linear relationship with  $\Delta T$ . This is unlikely to be the case, as ventilation heat loss is likely to increase the greater the  $\Delta T$  due to convection, stack and pressure effects.

The tracer gas decay method involves introducing an inert tracer gas into the building and measuring the concentration of the gas inside the building at specific time periods throughout the co-heating test. The tracer gas decay method will give a direct measure of the background ventilation rate averaged over the decay period (Roulet and Foradini 2002).

The constant concentration gas method involves introducing an inert tracer gas into the building and measuring the rate at which the tracer gas needs to be introduced into the building to maintain a specific concentration. This gives real time data on the ventilation rate for the duration of the co-heating test.

### **4.3 Recommendations for reliable results**

Currently the co-heating method experiences limited use mainly as a research tool in the UK, whilst there are examples of use in other locations (e.g. Masy, 1985). Examples exist of both how co-heating and additional evaluation tools can improve both our fundamental understanding of building heat loss (Lowe, 2007), and also provide effective feedback to developers to improve actual performance (Wingfield et al., 2011; Miles-Shenton et al., 2011). However, despite acknowledgement of the benefits more widespread testing could yield, further application has been limited for a number of reasons. In particular, the issues collected in this section need to be considered when planning to undertake a co-heating test.

#### **4.3.1 TESTING PERIOD**

The period within the year in which testing should be undertaken is dictated by the requirement to obtain a sufficiently large indoor-outdoor temperature difference  $\Delta T$  (generally 10 K or more). Consequently, the co-heating test should be carried out in the winter months. An added advantage of undertaking the tests during this period is that the effects of solar radiation are also minimised. This is to minimise the risk of the temperature within any of the south-facing rooms increasing above the mean set-point temperature within the dwelling due to the effects of solar gains.

#### **4.3.2 DURATION OF THE TEST**

Careful consideration must also be given to the duration of the co-heating test. The amount of time required to undertake a co-heating test can vary considerably and is dependent upon a range of factors. Such factors include: the thermal characteristics of the dwelling, the amount of residual moisture contained within the fabric of the dwelling, external environmental conditions, the time taken for the dwelling to become heat saturated and the objectives of the test. Ideally, the test should be undertaken for a sufficient period of time to enable there to be a number of data points plotted on the power versus  $\Delta T$  graph, at as wide a range or spread of  $\Delta T$  's as possible, such that an appropriate regression coefficient can be obtained for the data.

Experience suggests that as a minimum, the test should be undertaken for one week after heat saturation of the dwelling has occurred. In most cases a test should be able to be undertaken in 2 to 4 weeks. However, generally speaking, the longer the testing period, the greater the potential spread of the data obtained, and the better the outcome.

Co-heating test data should be collected 24 hours a day during the length of the test. Only measuring night-time data, say from 6pm to 6am, is not advised, as it tends to ignore mass effects. This can be particularly problematic in heavyweight dwellings.

#### **4.3.3 THE DETERMINATION OF DAILY AVERAGED DATA**

The analysis of co-heating data is normally undertaken using the average of the daily data, where daily data is defined as that data recorded over the period 00:00 to 23:59 inclusive. Analysing the data using daily figures will tend to smooth out the short-term (daily) effects of thermal mass and diurnal variations in temperature and solar radiation. By averaging the data over the period 00:00 to 23:59 inclusive it is assumed that all of the solar radiation

absorbed by the fabric of the dwelling is re-radiated back to the space by midnight of the day in which it was absorbed. This may be true in buildings of lightweight or even medium weight construction, but is unlikely to be true in dwellings of heavyweight construction. In such dwellings, it may be more appropriate to average the daily data over the period 06:00 to 05:59 inclusive, although it is recognised that in some dwellings, it may take more than a day for all of the absorbed thermal radiation from one day to be re-radiated back to the space.

#### **4.3.4 BUILDING TYPE AND FORM**

Careful consideration has to be given to the type, the form and the method of construction used on the dwelling that is to be tested. In dwellings that have a large number of relatively small rooms, additional equipment may need to be installed (fan heaters and/or air circulation fans) to ensure that the mean elevated temperature is achieved within all of the rooms within the dwelling. In dwellings that comprise two or more floors, difficulties can be encountered maintaining the mean elevated temperature throughout the dwelling, due to stack effects. Additional air circulation fans may need to be positioned within the dwelling to blow any warm air that is naturally rising up through the dwelling back down to the lower floors to enable adequate mixing of the internal air.

One of the most difficult dwelling forms to undertake a co-heating test on is an apartment. When testing apartments, careful consideration needs to be given to any heat loss that may occur through any party elements of construction (such as party walls, party floors, etc.) or to any unoccupied spaces (such as stairwells, communal areas, etc.), which are often not heated. Ideally, access to adjacent apartments or spaces should be obtained to maintain these spaces at the same mean elevated internal temperature as the test apartment.

In apartments that have a small proportion of external envelope area in relation to floor area, the heat loss from the apartment may be so low that it is difficult to obtain a reliable co-heating test result, due to the influence of various external factors, such as solar gains.

#### **4.3.5 WIND SPEED AND DIRECTION**

Wind speed and wind direction can have an impact on the results obtained from a co-heating test. The effect that these will have on the test result will be dependent upon a number of factors. These include: the airtightness of the test dwelling, the distribution of the leakage paths within the dwelling, orientation of the dwelling, location and the effects of any sheltering. In some cases, it may be possible to account for wind speed by introducing wind speed as an additional independent variable within a multivariate linear regression analysis. However, experience suggests that attempting to correct for wind speed and direction is inherently problematic due to the number of complex interrelated variables involved.

## **4.4 References**

1. Balcolombe, Douglas J., 1992. *Passive Solar Buildings*, MIT.
2. Bauwens, G. and S. Roels. 2014. Co-heating test: a state of the art. *Energy and Buildings* 82, 163-172.
3. Everett, R. Horton, A. and Doggart, J. 1985a. *Linford Low Energy Houses*. Open University Energy Research Group, Milton Keynes, UK.
4. Everett, R. 1985b. *Rapid Thermal Calibration of Houses*. Technical report ERG 055, Open University Energy Research Group, Milton Keynes, UK.
5. Liddament, M.W. 1996. *A guide to energy efficient ventilation*. Air infiltration and ventilation centre AIVC, [www.aivc.org](http://www.aivc.org).
6. Lowe, R.J., J. Wingfield, M. Bell. 2007. Evidence for significant heat losses through party wall cavities in load-bearing masonry construction, *Building Services Engineering Research and Technology* 28 (2) 161–181.

7. Masy, G., 1985. "Application de la méthode de la signature thermique à la maison de Bertem et à l'immeuble des Acacias : établissement des bilans thermiques et analyse de la régulation" IEA-ECBCS, Annexe XI.
8. Miles-Shenton, D ., Wingfield, J., Sutton, R. & Bell, M. (2010) Temple Avenue Project Part 1 – Evaluation of Design and Construction Process and Measurement of Fabric Performance of New Build Dwellings, Report to Joseph Rowntree Foundation, Leeds Metropolitan University, Leeds
9. Roulet, C-A. & Foradini, F. 2002. Simple and Cheap Air Change Rate Measurements Using CO<sub>2</sub> Concentration Decay, International Journal of Ventilation, Volume 1(2), 39-44
10. SAP, 2009. The Government's Standard Assessment Procedure for Rating of Dwellings, Watford, United Kingdom, pp.208.
11. Siviour, J. 1981. Experimental Thermal Calibration of Houses. Technical report for the Electricity Council Research Centre, Chester, United Kingdom.
12. Sonderegger, R. C. Condon, P. E. and Modera, M. P. 1979. In situ measurements of residential energy performance using electric co-heating. ASHRAE Transactions, Vol. 86 (I), 1980. LBL-10117.
13. Subbarao, K. Burch, J. D. Hancock, C. E. Lekov, A. and Balcomb, J. D. 1988. Short-Term Energy Monitoring (STEM): Application of the PSTAR Method to a Residence in Fredericksburg, Virginia. TR-3356. Colorado, USA, Solar Energy Research Institute.
14. Wingfield, J., D. Johnston, D. Miles-Shenton, M. Bell. 2010. Whole House Heat Loss Test Method (co-heating), Centre for built environment, Leeds Metropolitan University, UK.
15. Wingfield, J., Bell, M., Miles-Shenton, D . & Seavers, J. (2010) Elm Tree Mews Field Trial – Evaluation and Monitoring of Dwellings Performance – Final Technical Report, Leeds Metropolitan University, Leeds
16. Johnston, D., D. Miles-Shenton, D. Farmer, J. Wingfield. 2013. Whole House Heat Loss Test Method (co-heating), Centre for built environment, Leeds Metropolitan University, UK.



## 5. Rapid measurement of heat transfer coefficient of whole buildings based on transient heating

G. Pandraud (Isover Saint-Gobain)

### 5.1 Test procedure

In order to overcome the relatively long test duration of co-heating tests, which is seen as a major drawback of the method, alternative test protocols have been developed that take short-term data as a starting point to estimate the heat transfer coefficient of a building. The STEM/PSTAR-method, developed in the 1980's by Subbarao et al. (1988), allowed to determine the statics as well as dynamics of a building from tests conducted over a period of a few days. More recently, the QUB method (Quick U-Value of Buildings), has been developed by the Saint-Gobain group in order to estimate, in a relatively short time (two nights at most), the sum of thermal transmission  $H_{tr}$  and infiltration/ventilation losses  $H_{ve}$ .

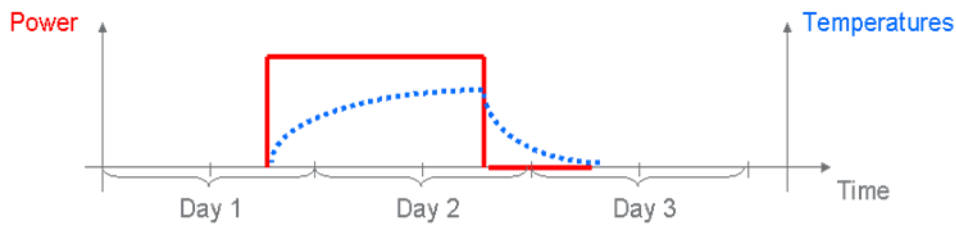


Figure 7.1: Schematic representation of the QUB-test procedure

The QUB-method has first been exposed and described in a patent (Mangematin et al. 2012a), and is discussed more in detail in this chapter. The method only uses the building temperature responses to two successive excitations of constant but different powers (generally, the building is first heated with a constant power and then cooled when the power source is stopped), see Figure 7.1. The external and internal temperatures of the building are measured during the entire period, and the time derivatives of the internal temperatures are calculated. If we note 1 and 2 each successive phase,  $\Phi_P$  the powers,  $\Delta T$  the difference between internal and external temperatures, and  $T'$  the time derivative of internal temperature  $dT/dt$ , then the measured heat transfer coefficient  $H$  is simply calculated by:

$$H = \frac{T'_1 \Phi_{P,2} - T'_2 \Phi_{P,1}}{T'_1 \Delta T_2 - T'_2 \Delta T_1} \quad (7.1)$$

This simple formula is easy to use, and requires only basic calculations which can be written in a spreadsheet.

There are only a few requirements for this method. All the measurements are made at night in an empty building in order to know the powers  $\Phi_{P,1}$  and  $\Phi_{P,2}$  with accuracy: electrical power is measured, solar or internal loads are considered negligible. Besides, the power must be in a range which is adapted to the external conditions. More precisely, if we can approximately estimate the value of  $H$ , for example with a heat transfer calculation, then the value of the parameter  $\alpha$  should hold approximately between 0.3 and 0.7, with:

$$\alpha = 1 - \frac{H \cdot (T_{i,0} - T_{e,1})}{\Phi_{P,1}} \quad (7.2)$$

and  $T_{i,0}$  the initial interior temperature, and  $T_{e,1}$  the mean exterior temperature during the first part of the test (typically heating). More details about the background of parameter  $\alpha$  is given in §7.2.

For accurate QUB measurements, it is essential that the input power is measured correctly. For this reason, the tests are done at night (to limit solar gains), in empty buildings (to limit internal gains), and the consumption of thermal powers is measured (for an electrical heating, intensity and tension have to be measured both to reduce uncertainty).

Similar as in the co-heating procedure, data treatment in QUB assumes homogeneous temperatures. It is possible to measure a temperature and calculate a heat transfer coefficient in each room, but if the temperatures of different rooms are all different, it can be difficult to assume that they are homogeneous inside each of the rooms. If they are not, the position of the temperature sensor can have a big influence on the results and lead to errors.

This is not an issue during co-heating tests, for instance, as in such quasi-static tests, temperatures can be regulated in each room, assuring a satisfying homogeneity. During a dynamic test, indoor temperatures will change at different speeds, depending on local powers, heat losses and internal heat transfers. A perfectly homogeneous heating can be approached by using a large number of low power sources (see §7.3).

## 5.2 Data analysis

The simplest model one can use to represent a building submitted to transient heat transfer is probably the lumped capacitance analysis with internal energy generation. It supposes that the interior of the building is at homogeneous temperature, that all heat transfer happens through an infinitely thin interface with homogeneous temperature, and that the exterior temperature is constant. Thus, it is an R-C model with only one resistance and one capacity. The well-known equation is (Mangematin et al. 2012b):

$$C \cdot dT = (\Phi_p - H \cdot \Delta T) \cdot dt \quad (7.3)$$

Where  $C$  is the internal heat capacity of the building (defined as the total energy needed to increase the interior temperature by 1 K, at a constant exterior temperature),  $\Phi_p$  the internal power brought by all heating sources inside the building and possibly the solar gain,  $H$  is the total heat transfer coefficient of the building and  $\Delta T$  is the difference between the interior and exterior temperatures.

If two separate experiments 1 and 2 are done, with two different powers, if we assume  $H$  and  $C$  to be constant during these two experiments and if we note  $T' = dT/dt$ , equation 6.1 can easily be demonstrated. Thus it is quite easy to calculate  $H$  from only two experiments if the temperature variation in time can be approximated by a linear function ( $T'$  constant), and if the temperature difference can be approximated by a constant average during part of the test period.

Of course, such a model is too crude to represent the real behaviour of a building. Thus, more complex models, first with 3 resistances and 2 capacities (Pandraud et al. 2013a), then with an infinite number of nodes (Pandraud et al. 2013b) have been used to prove that after a few hours with a constant heating power, the temperatures evolve as if the building had only one time constant. Hence, the model with one  $R$  and one  $C$  is assumed to be valid, and equation 7.1 can be used.

Other investigations have shown that if the duration of the heating period is equal to that of the cooling period ( $t_1 = t_2$ ), the tests can be accurate even if the total duration is less than 8 h, even as short as 1 h (Pandraud et al. 2014). To explain this effect, a different model has been developed, in which the envelope is represented by a multi-layer wall in which the heat transfer is 1-dimensional, but there is no limit on the number of layers. This problem is then solved by a quadruple approach.

Some assumptions are made in order to simplify the calculations:  $t_1 = t_2$ ; the external temperature is supposed to be constant during each phase; the QUB test is assumed to start from steady-state conditions; and the power dissipated during the cooling phase is negligible. The result of such a model can be written in a semi-analytic expression of  $H_{QUB}$ , the measured value of the heat transfer coefficient, as a function of its theoretical value  $H$ , a parameter called  $\alpha$ , as defined in equation 7.2, a function  $f(\alpha)$ , which depends on  $\alpha$  and on the heating duration  $t_1$ , and on the resistances  $R_i$  and the capacitances  $C_i$  of the model (i.e. of their repartition in the wall):

$$H_{QUB} = \frac{H}{1 - \alpha^2 f(\alpha)} \quad (7.4)$$

More details about the origin of this equation, how it is calculated and what it means are explained by Pandraud et al. (2014).

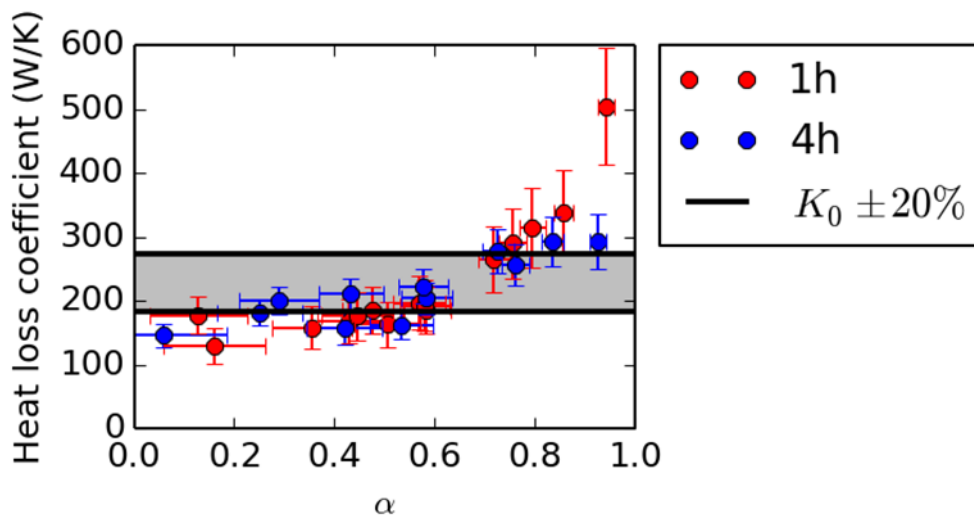


Figure 7.2:  $H_{QUB}$  vs.  $\alpha$  (Energy House Salford); 1 h and 4 h are the heating phase durations (half the total test duration);  $K_0$  is the reference value for the heat transfer coefficient  $H$  as obtained in steady state tests.

Equation 7.4 predicts that at low values of  $\alpha$ ,  $H_{QUB} = H$ , but that  $H_{QUB}$  increases with  $\alpha$  and can reach very high values when  $\alpha$  is close to 1 (although  $\alpha$  does not have theoretical bounds, its value is usually in the range 0-1, except when specific experimental conditions are reached, generally on purpose, in order to fully study its influence). This result has been tested both numerically and experimentally, and all results tend to the same conclusions. Figure 7.2 presents as example a study of the influence of  $\alpha$  on  $H_{QUB}$  made in the Energy House at the University of Salford.

The three main conclusions of the measurements are:

- as predicted, the value of  $H_{QUB}$  increases for high  $\alpha$  and overestimates the steady-state reference  $H$  ( $K_0$  in the figure),
- as predicted, the overestimation is reduced by increasing the test duration,

- contrary to what is predicted, low  $\alpha$  values can also lead to errors, in this case underestimations.

The third conclusion is not derived from the model we use, but numerical results tend to show that this is due to the hypothesis of initial steady state which is not accurate in practice. The numerical results confirm the experimental observations, both the large overestimation at high  $\alpha$  values and relatively smaller underestimations at low  $\alpha$  values. They show that, any value of  $\alpha$  between approximately 0.3 and 0.7 results can be described as good. This is true in this particular case but has been shown to be also true in other cases, for different construction types (Pandraud et al. 2013a).

### 5.3 Recommendations for reliable results

The heat sources chosen by Saint-Gobain are heating mats of a 112.5 W nominal power. Depending on its size, 20 to 60 mats are typically required for a single family house. These mats can be placed horizontally, as in a simulation of an underfloor heating system, but this has problematic consequences. It both heats the air and the floor, in proportions that might not be reproducible and have even been seen to change during a single test, leading to sudden air temperature variations.

To solve this problem, another use of these mats has been tested, with very interesting results. Instead of being put horizontally on the floor, they have been rolled and placed vertically (Fig. 7.3). This way, the heat exchange with the ground is minimal. Almost all of the heat power is dissipated in the air by natural convection (not really by radiation to the walls, as the mats are covered by an aluminium layer). This has led to a much better reproducibility and regularity.

With the mats thus placed, it is much easier to have a homogeneous interior temperature with smooth evolutions in time, which is rather important for a method that relies on slope calculations. Those slope calculations, and all data evaluations in general, can be done simply with software like MS Excel, for instance, but it is important that the periods considered for this evaluation are chosen appropriately.

First of all, as has been already explained, it is important that the chosen heating duration and the cooling duration be equal. Besides, the values are not evaluated at a single point, but over a time period. So to have identical durations, each data analysis period must start and end at the same time relative to the phase's beginning. For example, if the heating starts at 7 pm and ends at 1 am (for a 6 h heating duration), and we decide to evaluate all data over a period of 2 h, then the heating data are evaluated between 11 pm and 1 am, and the cooling data are evaluated 6 h later, between 5 am and 7 am. Thus, the data periods have the same duration and are both situated between 4 and 6 hours after the starts of their respective phases.

When these choices are made, it is only a matter of averaging interior and exterior temperatures as well as powers during these two periods and calculating the appropriate temperature slopes, to apply equation 7.1. In order to reduce the uncertainty, it is possible to evaluate different values of  $H$  for instance by checking the values for evaluation periods of 1.5, 2.0, and 2.5 h and averaging the values. It is also possible to weigh these values depending on criteria of quality of the correlation between temperature and time. There is no absolute rule for this aspect; any mathematical method enabling a better evaluation of the experimental temperature derivative can be used.



*Figure 7.3: Vertically rolled heating mats*

## **5.4 Application examples**

The QUB method has been tested in several reference cases. A reference case is a building in which the heat transfer coefficient measured according to the QUB-method has also been evaluated in another way, preferably with a lower uncertainty than the QUB method. Several of these validation cases have been made. They are of three types: virtual (simulated) buildings for which the exact heat loss can be calculated precisely; reference buildings in which steady-state can be achieved and the heat loss can be evaluated with a very low uncertainty; and real buildings for which it can be very difficult to have reference values.

### **5.4.1 VIRTUAL BUILDINGS**

In the case of QUB, the first feasibility tests have been made by comparing QUB results with reference values on the TRNSYS software. Some results for two-night tests are for instance presented by Alzetto et al. (2014). In this case, a building (single family house, 109 m<sup>2</sup>, interior insulation) has received the weather file corresponding to the city of Rennes (France), and every week of the year, a virtual QUB test has been made. All 52 values have been compared with the reference value obtained by putting the house in steady-state (weather file corresponding to a constant exterior temperature without solar radiation). The reference value predicted is 143 W/K, and all values defined by the QUB procedure are included between 136 and 167 W/K, for an average of 150 W/K (+ 5%) and a maximal deviation of 17% (Figure 7.3). It is clear that 90 to 95% of  $H_{QUB}$  values are included in  $H \pm 10\%$ .

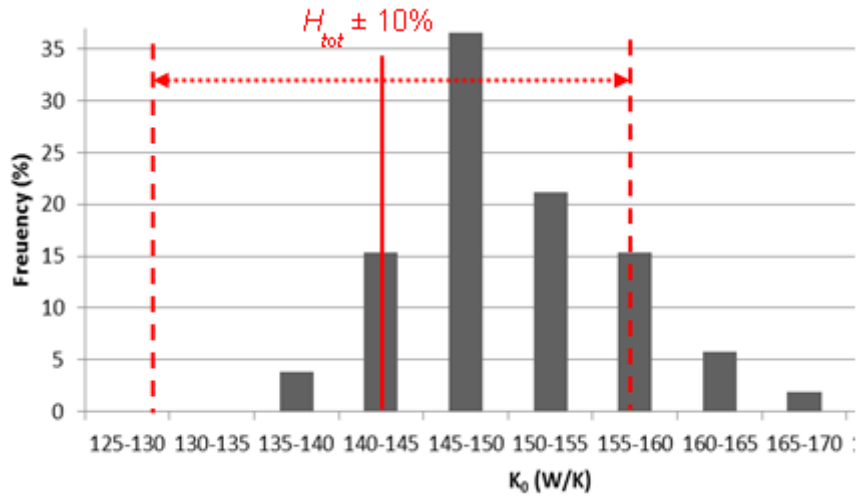


Figure 7.3: Distribution of  $H_{QUB}$  vs. reference value  $H_{tot}$  obtained in TRNSYS

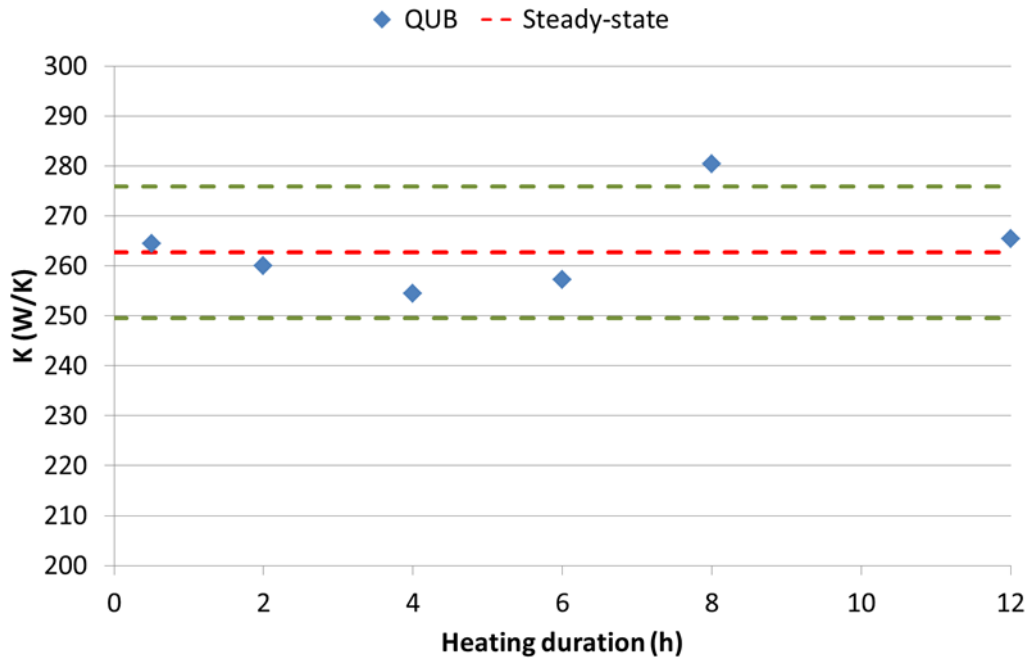


Figure 7.4:  $H_{QUB}$  vs.  $H$  measured in steady-state as a function of heating duration (data obtained in Salford Energy House)

#### 5.4.2 REFERENCE BUILDING: THE ENERGY HOUSE AT THE UNIVERSITY OF SALFORD

The Energy House at the University of Salford is a unique experimental facility in which a typical Victorian house has been reconstructed inside a climatic chamber, enabling accurate measurements of its heat loss in different conditions (Janssens 2016). For instance, figure 7.4 shows that  $H_{QUB}$  can be measured with a good reproducibility even when the test duration is strongly reduced (the green dashed lines indicate the steady-state value  $\pm 5\%$ ) (Pandraud et al. 2014). Figure 7.5 presents the very good concordance between results of QUB tests (8h total duration) and co-heating tests (performed by Leeds Metropolitan University, Farmer et al. 2014). The results are all very close, except maybe for the second test on Fig. 7.5, which can be explained by an experimental error: the test duration was in this case 1h instead of 8h.

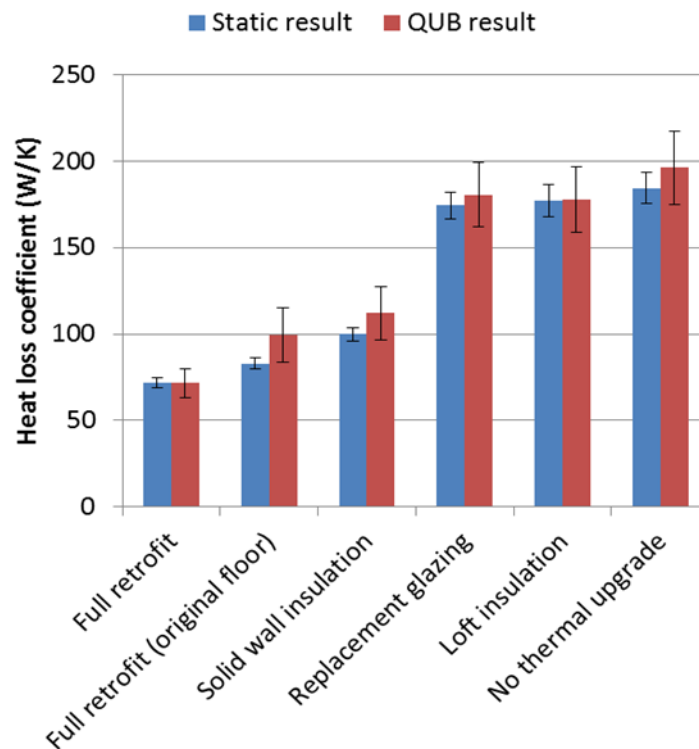


Figure 7.5: Comparison between QUB and co-heating results obtained at Salford Energy House

#### 5.4.3 REAL BUILDINGS

The main difficulty with real buildings is that a validation requires another estimation of the building heat loss. The simplest way to do this is with co-heating tests, which still require several weeks of measurements. Some tests have been done in small scale buildings, like bungalows, or in real houses, but none have been published yet. On the other hand, feasibility and reproducibility measurements have shown very good results, for instance in Pandraud et al. (2013a) where dispersions, even between measurements done in summer and winter, have been very low, with standard deviations inferior to 5%.

Besides, real buildings can be used to study the influence of other factors by successive measurements. For instance, the influence of air flow rate (through ventilation / infiltrations) has already been analysed this way by Pandraud et al. (2013a).

## 5.5 References

1. Alzetto F, Gossard D, Pandraud G. 2014. Mesure rapide du coefficient de perte thermique des bâtiments, Congrès Sciences et Technique Ecobat, 19-20 mars 2014, Paris.
2. Farmer D, Brooke-Peat M, Miles-Shenton D, Cuttle C, Gorse C. 2014. Saint-Gobain Energy House Thermal Upgrade Testing, Technical Report, Leeds Sustainability Institute, Leeds Metropolitan Institute (renamed Leeds Beckett University) Unpublished. Quoted from Gorse C, Miles-Shenton D, Farmer D, Fletcher M, Glew D, Stafford, Parker J, The Gap Between Calculated and Real Performance: Experiences from the Field and the Measures Required to Address the Difference, Proceedings of the Real Building Energy Performance Assessment Seminar, April 16th, 2014, Gent, p.7-21.
3. Inventory of full scale test facilities for evaluation of building energy performances (A. Janssens, ed.). 2016. IEA EBC Annex 58, Subtask 1, Final report.
4. Mangematin E, Pandraud G, Gilles J, Roux D. 2012a. Determination of the heat loss coefficient of a premises, Saint-Gobain Isover, WO 2012/028829 (A1), 2012.03.08.
5. Mangematin E, Pandraud G, Roux D. 2012b. Quick measurements of energy efficiency of buildings, C.R. Physique 13 (2012) 383-390.
6. Pandraud G, Mangematin E, Roux D, Quentin E. 2013a. QUB: a New Rapid Building Energy Diagnosis Method, Proceedings of Clima 2013, 11th REHVA World Congress, Prague, Czech Republic, June 16th-19th.
7. Pandraud G, Fitton R. 2013b. QUB: Validation of a Rapid Energy Diagnosis Method for Buildings, Free Paper presented at IEA – ECBCS – Annex 58 – ST3, June 9th, 2013, München.
8. Pandraud G, Gossard D, Alzetto F. 2014. Experimental optimization of the QUB method, Free Paper presented at IEA – ECBCS – Annex 58 – ST2, June 14th, 2014, Gent.
9. Subbarao, K., J. Burch, C. Hancock, A. Lekov, J. Balcomb. 1988. Short-Term Energy Monitoring (STEM) – Application of the PSTAR Method to a Residence in Fredericksburg, Virginia, Technical Report, Solar Energy Research Institute. Prepared for the U.S. Department of Energy, Contract No. DE-AC02-83CH10093.

## 6. Estimation of the energy signature of buildings in use based on energy use monitoring

C. Giaus (INSA de Lyon), E. Himpe (UGent)

### 6.1 Test procedure

The energy use data of buildings that are in use, are typically collected on a monthly or yearly basis, e.g. for billing purposes. Moreover, new and refurbished buildings are more and more equipped with energy monitoring systems (e.g. in Building Energy Management Systems) that record energy use data and related parameters at higher frequencies (e.g. one per hour, once per 15 minutes...). Combined with climatic data, these data may be used to assess the energy performance of the building based on a so-called energy signature model, that is the relation between the energy use and environmental parameters, typically the outdoor temperatures (Westergren 1999, Santamouris 2005). Simplified static models use the regression of energy consumption over the climatic data to obtain an energy signature.

This relation may be used to evaluate the overall heat transfer coefficient of the building represented by the regression coefficient of the energy use-external temperature relation, divided by the external surface, and the base temperature, which is related to heat gains. The overall heat transfer coefficient and the base temperature are simple concepts useful in economic analysis of energy performance or in energy labelling of buildings (Richalet 2001). The energy signature may be used to diagnose the energy performance of the building and to make meteorological corrections of the energy consumption. They also enable to check the design performance against real data and during normal operation to compare the building performance in different years.

### 6.2 Data analysis

#### 6.2.1 RELATION BETWEEN OUTDOOR TEMPERATURE AND ENERGY LOSS

The thermal power for heating a building may be written as:

$$\Phi_{P,H} = H(T_i - T_e) - \Phi_g \quad (8.1)$$

Where  $H$ , the global heat transfer coefficient of the building, takes into account the transmission and the ventilation heat losses,  $T_e$  is the outdoor temperature,  $T_i$  is the uniform internal temperature of a building zone, and  $\Phi_g$  are the heat gains from sun, internal sources (e.g. occupants, lights) and other zones (ASHRAE 2013). More generally,  $\Phi_g$  may include the effects of thermal inertia which makes equation 8.1 applicable in dynamic regime. The outdoor temperature for which the building at indoor temperature  $T_i$  is in thermal balance with its environment, without heating or cooling, is called base temperature  $T_b$  and is related to the heat gains:

$$\Phi_g = H(T_i - T_b) \quad (8.2)$$

In thermally controlled buildings, the indoor temperature is quasi-constant. Heating is needed only when the outdoor temperature is lower than the base temperature. The thermal power for heating the building is then:

$$\Phi_{P,H} = H[T_b - T_e]\delta_h \quad \text{with} \quad \delta_h = \begin{cases} 1, & \text{if } T_e < T_b \\ 0, & \text{if } T_e \geq T_b \end{cases} \quad (8.3)$$

The energy needed to heat the building during the time interval  $(t_2-t_1)$  is then:

$$Q_H = \int_{t_1}^{t_2} H[T_b - T_e(t)]\delta_t dt \quad (8.4)$$

Or, when considering a fixed time interval  $\Delta t$ , for example of one hour, and taking the mean of the variables during this interval:

$$Q_H = H(t)(T_b(t) - T_e(t))\Delta t \quad (8.5)$$

In real buildings both  $H$  and  $T_b$  may vary in time. Representing the energy use data,  $Q_H$ , as a function of the mean outdoor temperatures will result in a cloud of data. As an example figure 8.1 shows in the upper panel the cloud of data of energy consumption for heating during the working hours (9:00 to 17:00) for a simulated office building (Ghiaus 2006). Each point represents the energy consumption for an hour and the mean outdoor temperature during that hour. The lower panel presents the histogram of the outdoor temperature constructed using bins of  $1^\circ\text{C}$ .

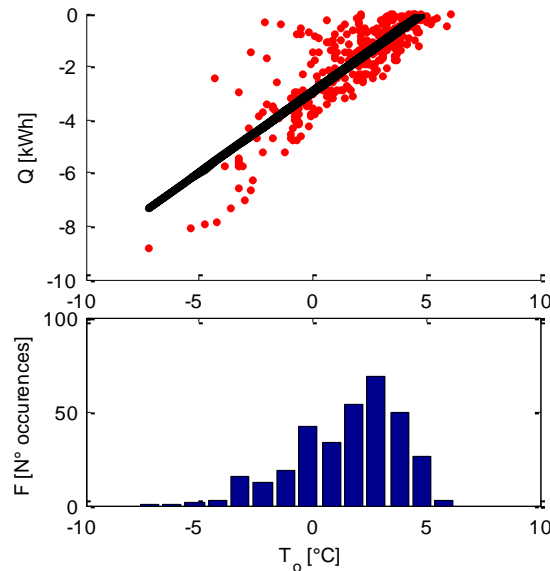


Figure 8.1: Example of hourly heating energy use ( $Q$ ) and outdoor temperature data ( $T_o$ ). Note that in this figure energy use assumes a negative value in case of heating. (Ghiaus 2006)

### 6.2.2 LINEAR REGRESSION AND CONDITIONS OF APPLICATION

By using linear regression, the data cloud may be approximated by the linear expression:

$$Q_H = \beta_0 + \beta_1 T_e \quad (8.6)$$

From equations 8.5 and 8.6 we obtain the model estimate of the global heat transfer coefficient of the building, and the base temperature, i.e. the outdoor temperature for which the energy use is zero:

$$H = -\beta_1 \quad (8.7)$$

$$T_b = -\beta_0 / \beta_1 \quad (8.8)$$

The assumptions made for linear regression are that the outdoor temperature,  $T_e$ , has a normal distribution and that the heat load,  $Q_H$ , is a random variable of mean  $\mu_Q = \beta_0 + \beta_1 T_o$ .

and homogeneous variance  $\sigma^2$ . These conditions imply that the residuals of the regressions should have a normal distribution with zero mean.

The assumptions made for linear regression are not always satisfied in real situations: the building is not air-conditioned at a constant temperature for the whole range of the outdoor temperature. Consequently, the outdoor temperatures which correspond to the heating period does not have a normal distribution. The application of linear regression may become more problematic when data on short time intervals are used, for instance obtained from energy monitoring systems. These data may be less correlated due to the influence of thermal lag and random, non-measured disturbances like occupancy, control actions, ventilation rates and solar gains that do not follow a normal (Gaussian) distribution. In literature a number of solutions are documented to mitigate these problems. Two examples are given here.

### 6.2.3 ROBUST REGRESSION OF HEATING LOAD CURVE BASED ON Q-Q PLOT

Ghiaus (2006) proposed a robust regression based on quantile – quantile plot to correctly estimate the parameters of the model. The points in a q-q plot represent quantiles of the data. Quantiles are values that partition a finite set of values into  $n$  subsets of equal size. The  $k$ -th quantile,  $P_k$ , is that value of the random variable  $x$  having  $N$  values, say  $x_k$ , which corresponds to a cumulative frequency of  $Nk/n$ . The quantile is called percentile for  $n= 100$ . The 25<sup>th</sup> and the 75<sup>th</sup> percentiles are called the first and the third quartiles. If the points in a q-q plot lie roughly on a line, then the distributions are the same, whether normal or not. Figure 8.2 shows an example of a q-q plot together with the corresponding histogram with real data collected in a French school building during a month of heating.

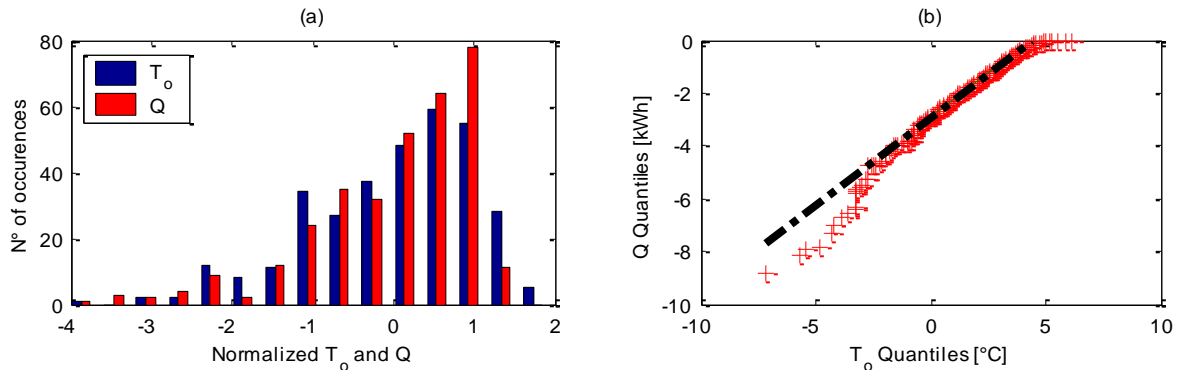


Figure 8.2: Outdoor temperature and the heating load have partially the same statistical distribution. a) histogram b) quantile-quantile plot (Ghiaus 2006)

A robust estimation of the linear relation between the outdoor temperature and the heating energy use may be done based on the central region of the q-q plot by considering data between the 1<sup>st</sup> and the 3<sup>rd</sup> quartile. If the two distributions are the same for this quantile range, then the coefficients of the model

$$\mathbf{Q} = a + b\mathbf{T}_o \quad (8.9)$$

are:

$$b = \sigma_Q / \sigma_{T_o} \quad (8.10)$$

$$a = \mu_{T_o} - b\mu_Q \quad (8.11)$$

#### 6.2.4 LINEAR REGRESSION CONSIDERING DYNAMIC AND SOLAR GAIN EFFECTS

Another method to improve the estimation of heat transfer coefficients based on linear regression of monitoring data is discussed by Danov et al. (2013). They suggest a linear regression-based method by using daily energy consumption and meteorological data. They show the total heat transfer coefficient can be estimated more precisely by explicitly including the accumulated heat and the solar gain in the building's energy balance through an estimation of the effective heat capacity and the net solar gain of the building.

The proposed method uses measurements of energy use, outdoor temperature and solar radiation that are integrated to daily data, because these are better correlated with respect to dynamic and solar radiation effects than higher frequency data, due to the thermal inertia of the building. The effective heat capacity of the building is evaluated by correlating the energy use and outdoor temperature changes from the previous day. The net solar gain of the building is assessed by analysing the data separated into groups by amount of daily solar irradiation. The calculation procedure then consists of the following steps:

1. from linear regression of all data points the initial H-value is estimated and the cross-point with the temperature axis is found;
2. by regression of the energy use changes and temperature changes between consecutive days the effective heat capacity of the building  $C_{eff}$  and subsequently the dynamic heat correction are determined from the average outside temperature of the actual (k) and previous day (k-1):

$$Q_{dyn} = C_{eff}(T_e^k - T_e^{k-1}) \quad (8.12)$$

3. by analysing the data by subsets for level of solar irradiation with applied dynamic heat correction, linear regressions with common cross-point (from step 1) are generated and the solar gain is determined;
4. the dynamic heat correction and solar gains are introduced in the energy balance and the corrected heat transfer coefficient H is determined.

### 6.3 Application example

This section gives an application example of the linear regression method considering dynamic and solar gain effects. In a case-study with 9 public buildings in Spain, Danov et al. (2013) estimated the total heat transfer coefficient in three ways:

3. without considering the dynamic and solar terms (basic method described in §8.2.2)
4. considering only the dynamic heat effect
5. considering the dynamic and solar gain effects

The results of the study indicated that in practically all of the cases the dynamic correction led to an improvement of the regression from the perspective of the determination coefficient values and the addition of the solar correction further improved the regressions' quality.

The observed corrections of the total heat transfer coefficient in the majority of cases led to an increase of the value within the range of 10%. The remaining scatter of the data was mainly due to building use factors, such as the inefficient control operation of the heating system (internal temperature variations), heating equipment malfunctioning and occupant activities and behaviour. Moreover the application showed that the estimates of the effective thermal capacity were considerably higher for intermittently heated buildings than for continuously heated buildings. This showed that the effective thermal capacity can be used as an indicator for the heating mode of the building.

The three parameters - the corrected total heat transfer coefficient, the effective heat capacity and the solar gain - can be used as performance indicators for specific

benchmarking in order to detect underlying building operational patterns and opportunities for energy savings based on daily data only.

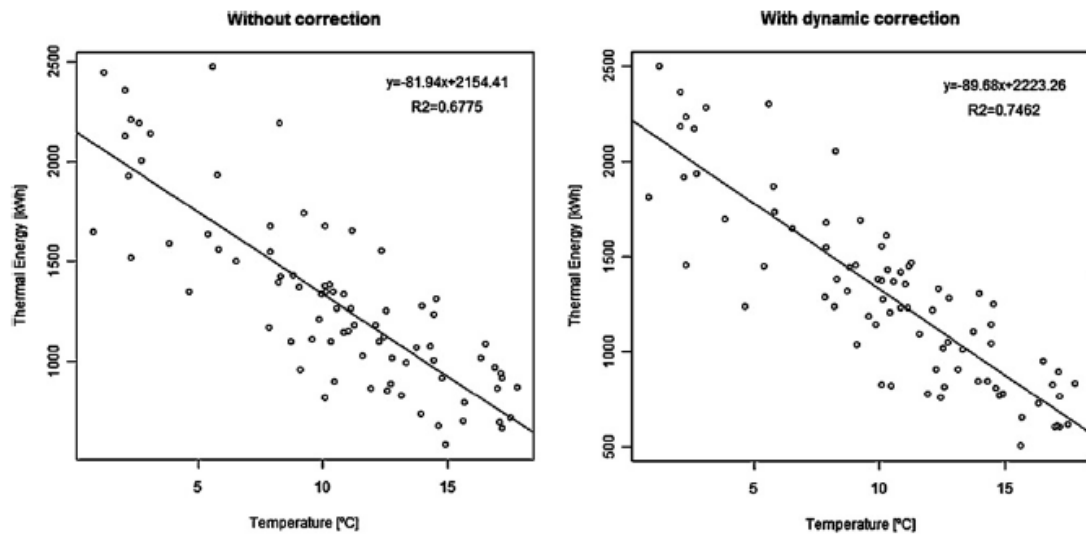


Figure 8.3: Total heat transfer coefficient determined from energy signature (daily data), with and without correction for the dynamic effect (Danov et al. 2013)

## 6.4 References

1. ASHRAE, Energy Estimating and Modeling Methods, in ASHRAE Fundamentals. 2013
2. Danov, S., J. Carbonell, J. Cipriano, J. Marti-Herrero. 2013. Approaches to evaluate building energy performance from daily consumption data considering dynamic and solar gain effects. *Energy and Buildings*, 57, 110-118.
3. Ghiaus, C. 2006. Experimental estimation of building energy performance by robust regression. *Energy and Buildings*, 38, 582-587.
4. Richalet, V., F.P. Neirac, F. Tellez, J. Marco, J.J. Bloem. 2001. HELP: methodology and present results. *Energy and Buildings*, 33, 229-233.
5. Santamouris, M. 2005. Energy performance of residential buildings : a practical guide for energy rating and efficiency. London: James and James.
6. Westergren, K.-E., H. Högberg, and U. Norlén. 1999. Monitoring energy consumption in single-family houses. *Energy and Buildings*, 29, 247-257.



# 7. Grey box modelling of buildings in use based on dynamic energy use data

P. Bacher (DTU)

## 7.1 Data analysis method

Analysing high-time resolution data measured in buildings requires modelling techniques which describe the heat dynamics of the building. Grey-box modelling is a modelling approach where prior physical knowledge are combined with data driven statistical modelling techniques (Bohlin and Graebe, 1995). Based on data with high time-resolution and a thoroughly developed framework for statistical inference using maximum likelihood techniques, dynamical systems can be modelled, and statistical testing, model selection and uncertainty estimation can be carried out. The models can be very detailed and both linear and non-linear effects can be modelled.

In a grey-box model a description of the heat dynamics is given with a set of continuous stochastic differential equations (SDEs) in combination with a set of discrete measurement equations. This forms a continuous-discrete stochastic state-space model. The SDEs forms a lumped element model description of the physical system based on heat transfer and the model parameters are directly interpretable as representing physical entities, e.g. the heat capacities and heat transfer coefficients of different parts of the building.

In this section first a description of a maximum likelihood scheme for parameter and uncertainty estimation in grey-box models is given, followed by a description of the required most basic set of measurements for grey-box modelling of a building. Then an outline of the output results and the advantages and drawbacks are discussed. Finally, a description of application studies with references are given.

### 7.1.1 MODEL STRUCTURE AND PARAMETER ESTIMATION METHOD

This section contains a condensed outline of a parameter estimation scheme for continuous-discrete time stochastic state space models. A detailed outline of the scheme is given by Kristensen and Madsen (2003) and Kristensen et al. (2004a). The scheme is implemented in the R package CTSM-R which is free and open source. The package and documentation can be found at the <http://ctsm.info>.

In the general case, the continuous-discrete stochastic state space model is a model that consists of a set of non-linear discretely, partially observed SDE's with measurement noise, i.e.:

$$dx_t = f(x_t, u_t, t, \theta)dt + \sigma(u_t, t, \theta)d\omega_t \quad (9.1)$$

$$y_k = h(x_k, u_k, t_k, \theta)dt + e_k \quad (9.2)$$

where  $t \in \mathbb{R}$  is the time variable;  $x_t \in X \subset \mathbb{R}^n$  is a vector of state variables;  $u_t \in U \subset \mathbb{R}^m$  is a vector of input variables;  $y_k \in Y \subset \mathbb{R}^l$  is a vector of output variables;  $\theta \in \Theta \subset \mathbb{R}^p$  is a vector of (possibly unknown) parameters;  $f(\cdot) \in \mathbb{R}^n$ ,  $\sigma(\cdot) \in \mathbb{R}^{n \times n}$  and  $h(\cdot) \in \mathbb{R}^l$  are non-linear functions;  $\{\omega_t\}$  is an  $n$ -dimensional standard Wiener process and  $\{e_k\}$  is an  $l$ -dimensional white noise process with  $e_k \in N(0, S(u_k, t_k, \theta))$ .

SDE's may be interpreted both in the sense of Stratonovich and in the sense of Itô, but since the Stratonovich interpretation is less suitable for parameter estimation (Jazwinski 1970), the

Itô interpretation is adapted. Furthermore, the diffusion term in eq. 9.1 is assumed to be independent of the state variables, because this renders parameter estimation more feasible.

### 7.1.2 PARAMETER ESTIMATION

The solution to eq. 9.1 is a Markov process and an estimation scheme based on probabilistic methods can therefore be applied to estimate the unknown parameters of the model in eq. 9.1-9.2, e.g. *maximum likelihood* (ML) or *maximum a posteriori* (MAP), where the latter can be applied if prior information about the parameters is available. Let:

$$\mathbf{Y} = [Y_{N_1}^1, Y_{N_2}^2, \dots, Y_{N_i}^i, \dots, Y_{N_S}^S] \quad (9.3)$$

be a set of S stochastically independent sequences of consecutive measurements, where:

$$Y_{N_i}^i = [y_{N_i}^i, \dots, y_k^i, \dots, y_1^i, y_0^i] \quad (9.4)$$

and let  $p(\theta)$  be a prior probability density function for the parameters. In the general case, point estimates of the parameters in 9.1-9.2 can then be found as the parameters  $\theta$  that maximize the posterior probability density function:

$$p(\theta | \mathbf{Y}) \propto \left( \prod_{i=1}^S p(Y_{N_i}^i | \theta) \right) p(\theta) \quad (9.5)$$

or equivalently:

$$p(\theta | \mathbf{Y}) \propto \left( \prod_{i=1}^S \left( \prod_{k=1}^{N_i} p(y_k^i | Y_{k-1}^i, \theta) \right) p(y_0^i | \theta) \right) p(\theta) \quad (9.6)$$

where the rule  $P(A \cap B) = P(A|B)P(B)$  has been applied in a successive manner to form products of conditional probability density functions.

### 7.1.3 UNCERTAINTY ESTIMATION

Since the parameter estimates are asymptotically normal distributed, and their covariance matrix can be approximated, the uncertainty (as the standard deviation) of each parameter can be found and t-tests can be used to test for significance, i.e. each parameter can be tested if it is significantly different from zero. An estimate of the uncertainty of the parameter estimates can be obtained by using the fact that by the central limit theorem the estimator is asymptotically Gaussian with mean  $\theta$  and covariance matrix:

$$\Sigma_{\hat{\theta}} = \mathbf{H}^{-1} \quad (9.7)$$

where the matrix  $\mathbf{H}$  is given by the elements:

$$h_{ij} = -E \left\{ \frac{\partial^2}{\partial \theta_i \partial \theta_j} \ln(p(\theta | \mathbf{Y}, y_0)) \right\}$$

for  $i, j = 1, \dots, p$ , and where an approximation to  $\mathbf{H}$  can be obtained from the elements:

$$h_{ij} = - \left( \frac{\partial^2}{\partial \theta_i \partial \theta_j} \ln(p(\theta | \mathbf{Y}, y_0)) \right) \Big|_{\theta = \hat{\theta}}$$

for  $i, j = 1, \dots, p$ , which is the Hessian at the minimum of the objective function. A measure of the uncertainty of the individual estimates can be obtained by decomposing the covariance matrix:

$$\Sigma_{\hat{\theta}} = \sigma_{\hat{\theta}} \mathbf{R} \sigma_{\hat{\theta}} \quad (9.8)$$

into  $\sigma_{\hat{\theta}}$ , which is a diagonal matrix of the standard deviations of the parameter estimates, and  $\mathbf{R}$ , which is the corresponding correlation matrix. The uncertainty information thus obtained

can subsequently be applied to perform tests of various hypotheses, e.g. to determine the significance of the individual parameters through t-tests.

The asymptotic Gaussianity (i.e. normal distribution) of the estimator allows t-tests to be performed to test the hypothesis:

$$H_0 : \theta_j = 0 \quad (9.9)$$

Against the alternative:

$$H_1 : \theta_j \neq 0 \quad (9.10)$$

i.e. to test whether a given parameter  $\theta_j$  is marginally insignificant or not. The test quantity is the value of the parameter estimate divided by the standard deviation of the estimate, and under  $H_0$  this quantity is asymptotically t-distributed with a number of degrees of freedom DF that equals the total number of observations minus the number of estimated parameters, i.e.:

$$z^t(\hat{\theta}_j) = \frac{\hat{\theta}_j}{\sigma_{\hat{\theta}_j}} \in t(DF) = t\left(\left(\sum_{i=1}^S \sum_{k=1}^{N_i} I\right) - p\right) \quad (9.11)$$

where, if there are missing observations in  $y_k^i$  for some  $i$  and some  $k$ ,  $I$  is replaced with the appropriate value of  $\bar{I}$ . To facilitate these tests,  $z^t(\hat{\theta}_j)$ ,  $j = 1, \dots, p$ , are computed along with the probabilities:

$$P\left(t < -|z^t(\hat{\theta}_j)| \wedge t > |z^t(\hat{\theta}_j)|\right), j = 1, \dots, p \quad (9.12)$$

More details about the statistical tests can be found in Ljung (1999) and Madsen and Holst (2000).

## 7.2 Model inputs and outputs

### 7.2.1 MEASUREMENTS

The following measurements are needed for a basic setup:

- Indoor air temperature ( $^{\circ}\text{C}$ ). A time series representative of the indoor air temperature in the building. Since the models are lumped and the heat capacities are constant the temperatures are directly describing the thermal energy accumulated in the lumped mediums. The measured indoor air temperature should therefore represent the average temperature of the indoor air.
- Heat input ( $\text{W}$ ). A time series with values of the heating power provided by heaters in the building.
- Ambient temperature ( $^{\circ}\text{C}$ ). A time series of the ambient temperature in the surroundings of the building.
- Global radiation ( $\text{W}/\text{m}^2$ ). A time series of the global radiation measured near the building.
- Wind speed ( $\text{m}/\text{s}$ ). A time series of the wind speed measured near the building. Furthermore the wind direction is important to measure.

In order to model a dynamical system it is necessary to excite the system such that the dynamic response can be modelled. The dynamic excitement must be designed to be in the frequency and operation range dependent on system response in order to maximize the level of information in the recorded data. Furthermore the inputs should be uncorrelated, hence the controllable inputs should be designed to achieve this. Sequences with such properties can be formed by several techniques, for example as by a PRBS (Godfrey, 1980) or a ROLBS. The controllable input in the presented setup is the sequence with which the heaters are controlled.

### **7.2.2 OUTPUT PARAMETERS**

A grey-box model is formed by a physical lumped parameter description of the system dynamics combined with a statistical model part. The parameters in the physical part are directly interpretable as representing the physical properties of the lumped elements. The typical parameters in the models are

- Heat transfer coefficients (or equivalently thermal resistances) between the lumped elements, for example from the interior to the ambient surroundings representing the H-value of the building.
- Effective heat capacities. The effective heat capacities of different parts of the building represented by the lumped elements, for example of the indoor air and the interior walls and furniture.
- Effective solar aperture. The effective area in which solar radiation enters the building.
- Wind induced infiltration. Parameters representing the effect of wind speed on infiltration.

The parameters are estimated in a maximum likelihood setting with a Kalman filter as described in Section 9.1. This scheme provides a range of statistical techniques to evaluate the performance of the model, for example the one-step ahead residuals are assumed to be white noise, which can be tested with the auto-correlation function and the cumulated periodogram. Furthermore, the Kalman filter minimize the impact of un-modelled effects on the parameters and time series plots of the one-step ahead residuals and the inputs are very useful for understanding model deficiencies. Kristensen et al. (2004b) suggest a systematic approach for improvement of grey-box models and Bacher and Madsen (2011) present a procedure for selecting and evaluating a suitable grey-box model for the heat dynamics of a building.

### **7.2.3 ADVANTAGES AND DRAWBACKS**

The main advantages of stochastic grey-box modelling are

- Continuous time physical description of the dynamics where parameters are directly physically interpretable.
- Can be applied for high time-resolution measurements, hence the testing period can be minimized.
- Maximum likelihood framework provides statistical techniques for assessment of the model performance and tests applicable for model selection. The setup furthermore provides techniques for pointing out model deficiencies.
- Models are highly extendable and can model complicated non-linear dynamical systems, providing detailed insights into the dynamics and energy performance of buildings.
- Multiple input and output models can be applied allowing detailed modelling based on experiments with advanced sensor setups.

The main drawbacks are:

- In the current modelling setup using the indoor air temperature as model output control over the heat input using a test sequence is required.
- Compared to black-box discrete ARMAX models (Jimenez and Madsen, 2008) (or a bit more simplified as ARX models), where the dynamics are modelled by discrete transfer functions in which the parameters cannot be directly physically interpreted, then the formulation and the selection of a suitable grey-box model is naturally complicated.

## 7.3 Application example

In this section a description of grey-box modelling of the heat dynamics of a building is presented. The experiments and data are described in full details in the report Bacher and Madsen (2010) and the modelling in the article Bacher and Madsen (2011). The R package CTSM-R is applied for the grey-box modelling. A two-state model is implemented, fitted and a model validation is carried out by analysing the one-step ahead residuals and the parameter estimates and uncertainties. Then the two-state model is extended to a three-state model, which is fitted and analysed, and compared to the two-state model with a likelihood ratio test, in order to determine if the three-state model is a more suitable model compared to the two-state model.

### 7.3.1 DATA

The data used in this example was measured in an office building which is part of the smart-grid experimental facility SYSLAB at DTU Elektro, Risø campus laboratory for intelligent distributed power systems in Denmark. The building is built in a lightweight wood construction. Time series of five minutes average values covering six days are used, plotted in Figure 9.1 from top to bottom:

- $T_i$  the average of all the indoor temperatures measured (one in each room in the building). The sensors were hanging approximately in the centre of each room ( $^{\circ}\text{C}$ ).
- $T_a$  the ambient temperature ( $^{\circ}\text{C}$ ).
- $\Phi_{P,H}$  the total heat input for all electrical heaters in the building (W).
- $\Phi_s$  the global solar radiation ( $\text{W}/\text{m}^2$ ).
- $W_s$  the wind speed (m/s) (not represented in Fig. 9.1).

The climate variables were measured with a climate station next to the building. The electrical heaters are controlled with a PRBS signal, which is composed of two periods: a PRBS with periods in one state between 20 minutes and 2 hours - that is Part One in Table 9.1 - and one period of a PRBS with periods in one state between 3.5 and 20 hours, it is Part Two in the table. Note the Part One is repeated.

*Table 9.1: Parameters for the single PRBS used for all heaters in Experiment 1. Note that Part One is repeated, i.e. as stated. The total length is 150 h = 6.25 days.*

Part	n	$\lambda$ , shortest period in one state	$n\lambda$ , longest period in one state	Total length
One	6	20 min	2 h	21 h
One	6	20 min	2 h	21 h
Two	5	3.5h	20 h	108 h

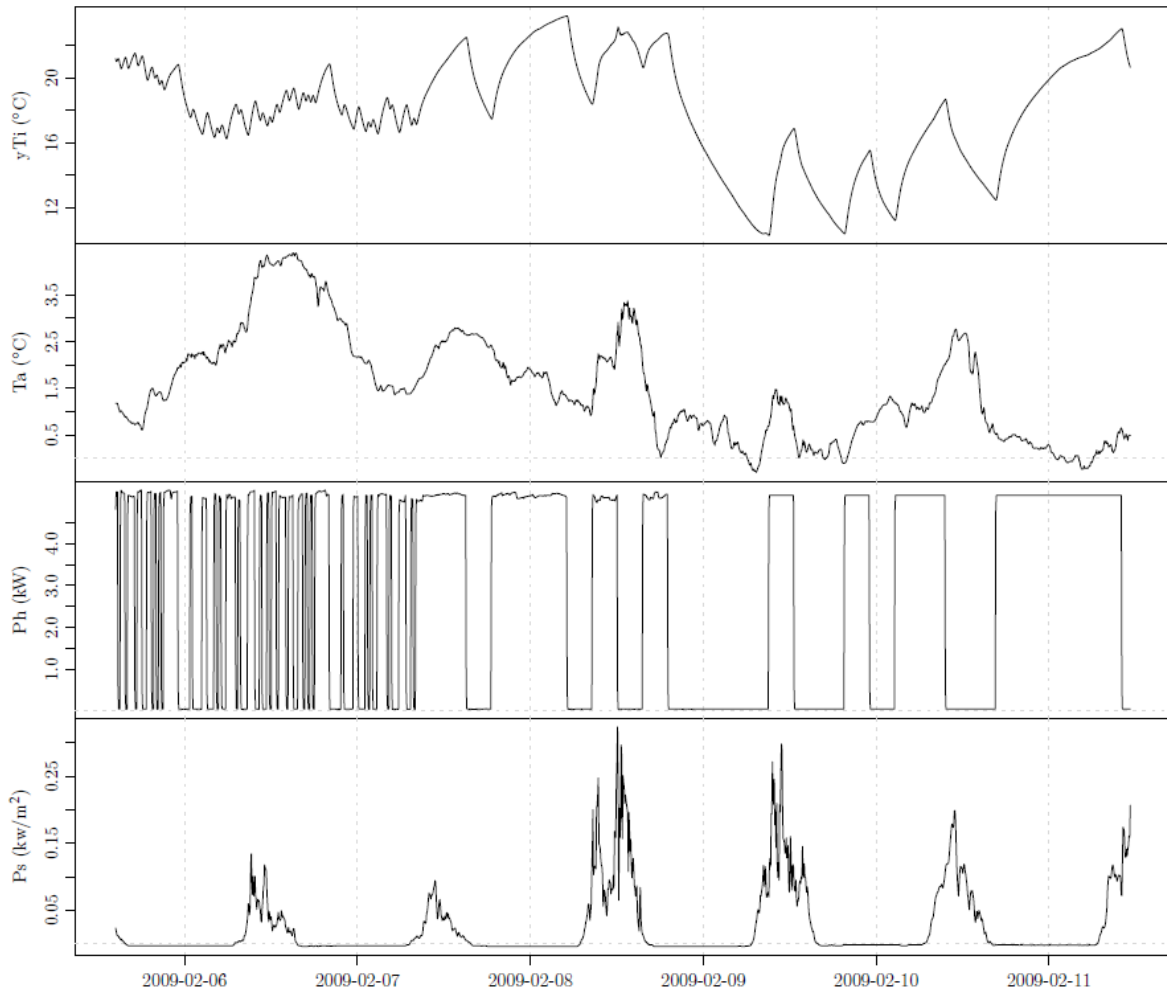


Figure 9.1: Plots of the data: indoor and ambient temperature, heat input, global solar radiation.

### 7.3.2 TWO-STATE GREY-BOX MODEL OF THE HEAT DYNAMICS OF A BUILDING

The two-state grey-box model  $Model_{TITe}$  illustrated with the RC-diagram in Figure 9.2 and defined by the system equations 9.13-9.14 together with the measurement equation 9.15 are specified in CSTM-R:

$$dT_i = \left( \frac{1}{R_{ie}C_i} (T_e - T_i) + \frac{1}{C_i} A_w \Phi_s + \frac{1}{C_i} \Phi_h \right) dt + \sigma_i d\omega_i \quad (9.13)$$

$$dT_e = \left( \frac{1}{R_{ie}C_e} (T_i - T_e) + \frac{1}{R_{ea}C_e} (T_a - T_e) \right) dt + \sigma_e d\omega_e \quad (9.14)$$

$$Y_k = T_{i,k} + e_k \quad (9.15)$$

The one-step ahead predictions and residuals are calculated and the auto-correlation function, the periodogram and the cumulated periodogram are plotted, see Fig. 9.3. Clearly, the residuals are not white noise and it is concluded that the model lacks in the description of the heat dynamics of the building. Considering the time series plot of the residuals (Fig. 9.4, first subplot), it becomes apparent that the dynamics of the system is poorly modelled in the short periods after level shifts in the PRBS heat input signal, i.e. every time the heaters are turned on and off. In the two-state model  $Model_{TITe}$  the heat from the heaters is flowing directly into indoor air and the thermal inertia of the heaters is not taken into account. This

leads to the idea of including a part in the model which represent the heaters, as carried out in the three-state model described in the following section.

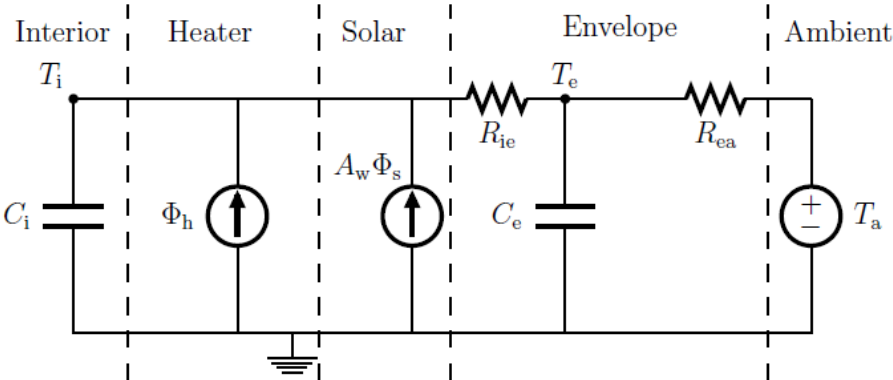


Figure 9.2: RC-network equivalent

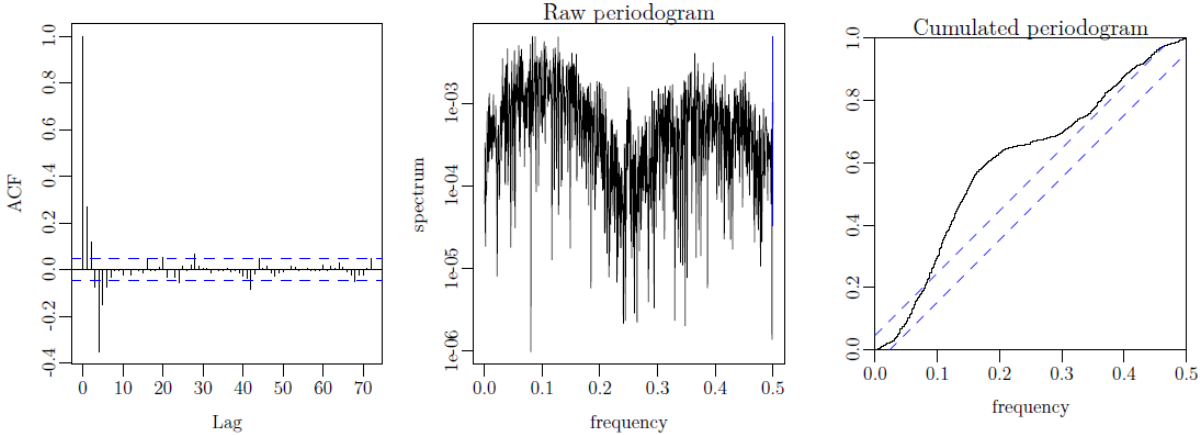


Figure 9.3: Plots of periodograms of two-state grey-box model

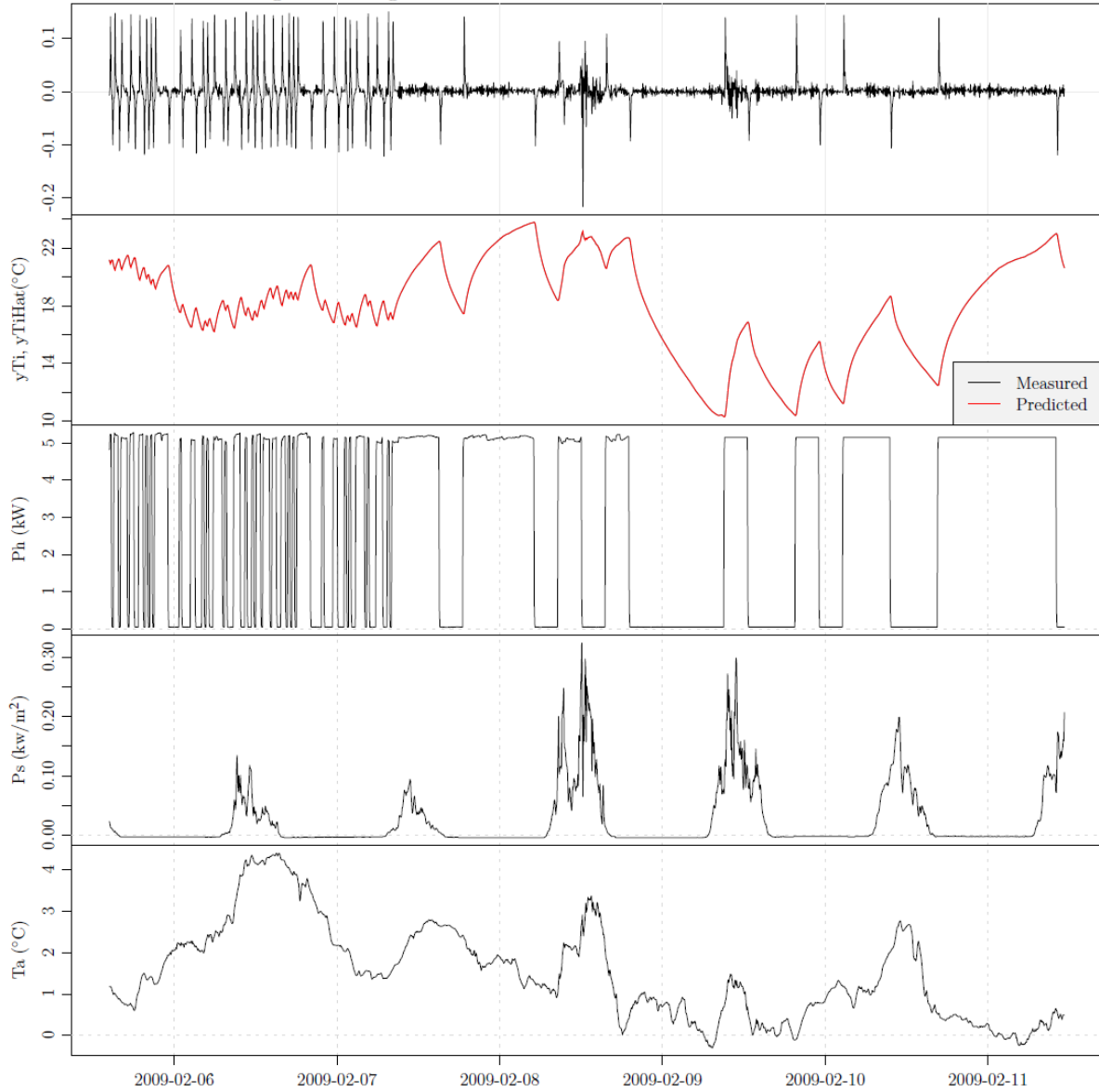


Figure 9.4: Time series plots of residuals (1<sup>st</sup> subplot [°C]), output (2<sup>nd</sup> subplot, measured and predicted indoor temperature values coincide) and inputs of two-state grey box model

### 7.3.3 THREE-STATE GREY-BOX MODEL OF THE HEAT DYNAMICS OF A BUILDING

In this section a three-state model is fitted to the data and the results are analysed. The model is an extension of the two-state, where a heat capacitor and a thermal resistance are added to represent the heaters in the building. A temperature state  $T_h$  representing the temperature of the heaters is included and the model equations become:

$$dT_i = \left( \frac{1}{R_{ie}C_i}(T_e - T_i) + \frac{1}{R_{ih}C_i}(T_h - T_i) + \frac{1}{C_i}A_w\Phi_s \right) dt + \sigma_i d\omega_i \quad (9.16)$$

$$dT_e = \left( \frac{1}{R_{ie}C_e}(T_i - T_e) + \frac{1}{R_{ea}C_e}(T_a - T_e) \right) dt + \sigma_e d\omega_e \quad (9.17)$$

$$dT_h = \left( \frac{1}{R_{ih}C_h}(T_i - T_h) + \frac{1}{C_h}\Phi_h \right) dt + \sigma_h d\omega_h \quad (9.18)$$

The RC-diagram in Fig. 9.5 is illustrating the model and it is denoted  $Model_{T_i T_e T_h}$ . The model is fitted (i.e. parameters are estimated) with CSTM-R and the autocorrelation and cumulated periodogram are plotted, see Fig. 9.6. Clearly, the one-step ahead prediction residuals have white noise properties, especially compared to the residuals for the two-state model. Finally, the plots of the time series confirm that the residuals are much closer to white noise. Studying the residuals a bit closer reveals that the 8'th and 9'th, have some shorter periods with direct solar radiation, and that the level of the residuals in these periods is increased. Therefore further expansion of the model could be focused on improving the part of the model, where the solar radiation enters the building.

Likelihood-ratio tests are very useful for determining whether a larger model is to be preferred over a smaller model (i.e. the smaller model is a submodel of the larger model), see Madsen and Thyregod (2010). Here a likelihood ratio test comparing the likelihood of the two-state model to the likelihood of the three-state model is used, see Bacher and Madsen (2011) for details. They show that the p-value is very low ( $<1E-16$ ) and thus the three-state model is preferred over the two-state model.

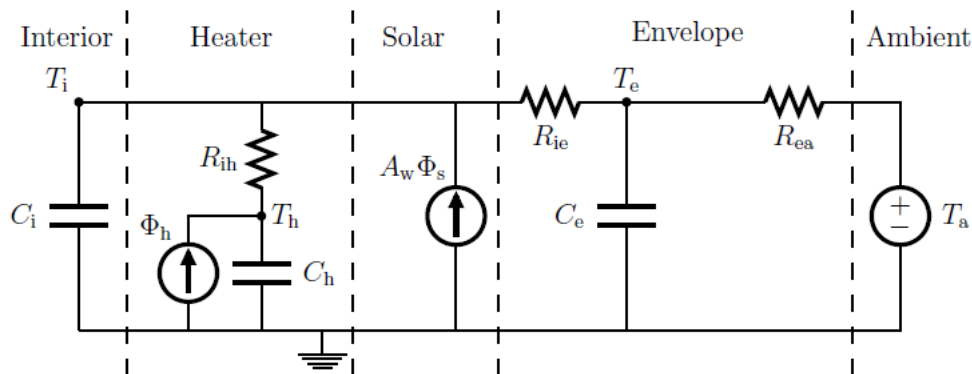


Figure 9.5: RC-network equivalent of the three-state model  $Model_{T_i T_e T_h}$

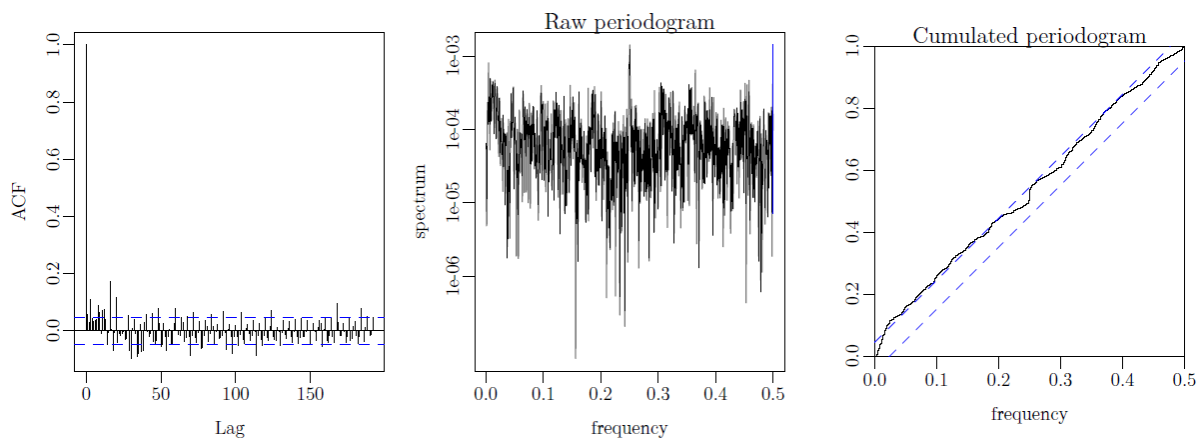


Figure 9.6: Plots of periodograms of three-state grey-box model

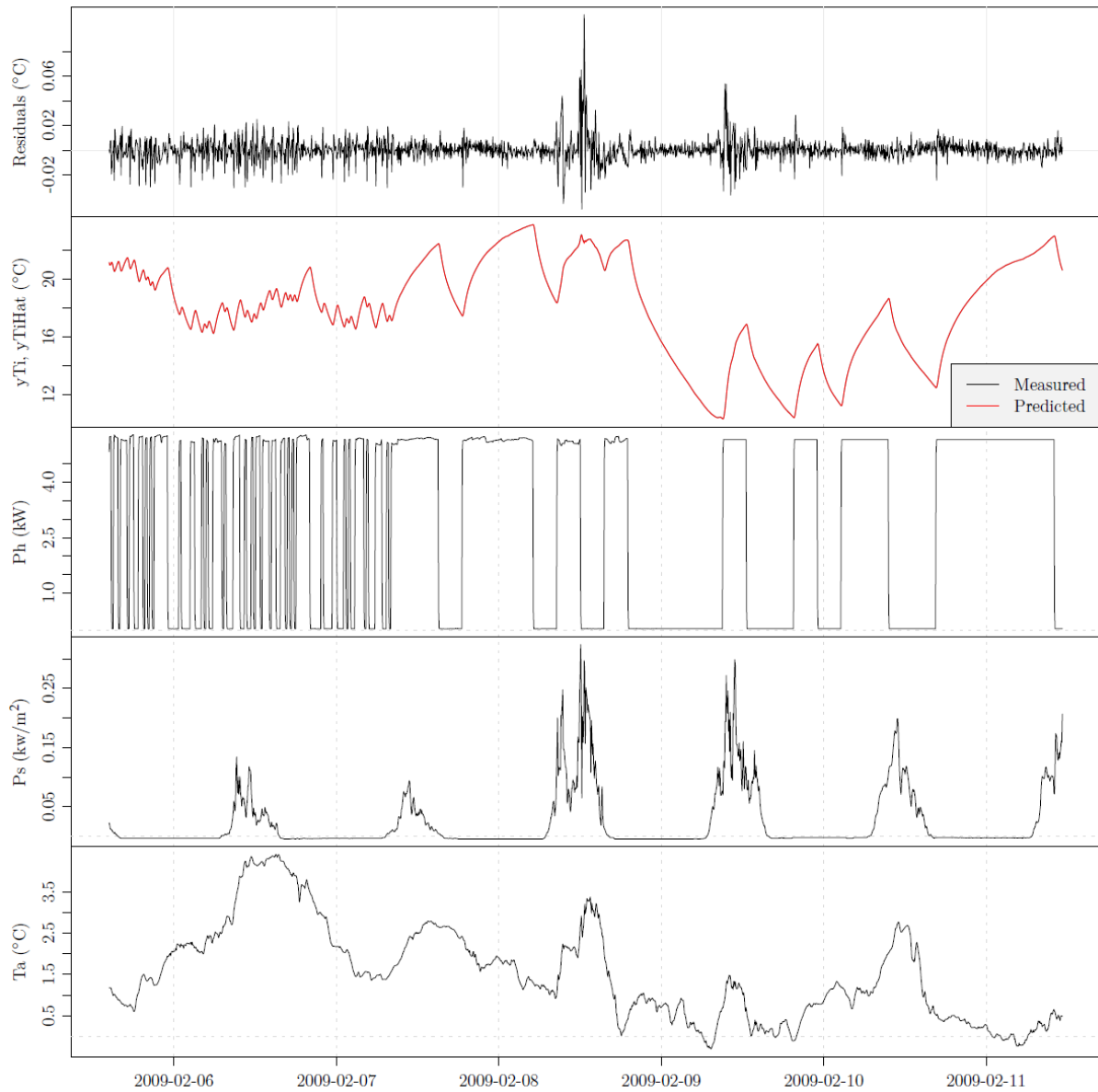


Figure 9.7: Time series plots of residuals (1st subplot [ $^{\circ}\text{C}$ ]), output (predicted indoor temperature, 2nd subplot, measured and predicted values coincide) and inputs of three-state grey box model

Table 9.2: The parameter estimates and the standard deviations The heat capacities,  $C$ , are in ( $\text{kWh/K}$ ). The thermal resistances,  $R$ , are in ( $\text{K/kW}$ ). The window area,  $A_w$ , is in ( $\text{m}^2$ ).

Parameter	Estimate	Standard deviation
$\hat{C}_i$	1.1	0.012
$\hat{C}_e$	2.9	0.14
$\hat{C}_h$	0.0014	0.00015
$\hat{R}_{ih}$	93	9.7
$\hat{R}_{ie}$	0.86	0.023
$\hat{R}_{ea}$	4.5	0.094
$\hat{A}_w$	5.6	0.26

### 7.3.4 PARAMETER ESTIMATES

In Table 9.2 the parameters and their standard deviations are listed. Clearly, the estimated value of thermal resistance between the heaters and the indoor air around 93 K/kW is not feasible from a physical perspective, which is also the case for the heat capacity of the heaters. The reason for these two values being not physically interpretable is that the actual heat transfer is in reality more complex than the linear approximation assumed in the RC-formulation. However, as found in the paper (Bacher and Madsen, 2011), further extension of the model can be carried out based on likelihood-ratio tests from the two-state and on to a four-state model, providing a better description of the dynamics. It is emphasized that the models are lumped linear approximations to the real system and care should be taken when interpreting the physical representation of each parameter, especially the smaller heat capacities in the present case.

The estimated total heat transfer coefficient  $H$  of the building is for the three state model simply calculated by eq. 9.19. The  $H$ -value is thus estimated to  $\hat{H} = 185.1$  W/K.

$$\hat{H} = \frac{1}{\hat{R}_{ie} + \hat{R}_{ea}} \quad (9.19)$$

However the estimate of its standard deviation cannot be calculated directly. The total  $H$ -value is a non-linear function of two normally distributed values, which means that the variance cannot be directly calculated. Two reasonable approaches can be applied: a linear approximation and a simulation approach. For the linear approximation the Jacobian is found as described in Jiménez et al. (2008) and used to calculate the variance of the estimated  $H$ -value to  $\hat{\sigma}_H = 3.1$ , which results in a 95% confidence interval  $\hat{H} \pm 1.96 \hat{\sigma}_H = [179.0, 191.2]$  W/K.

For the simulation approach a set of multivariate normal values based on the estimates of the  $R$  values are generated. The  $H$ -value is then calculated for the generated values and the 2.5% and 97.5% quantiles are estimated as the confidence interval  $\text{conf}_{\text{sim},H} = [179.2, 191.4]$ .

## 7.4 Applications in literature

The following is a list of applications of grey-box modelling for energy performance assessment of buildings and building components.

Madsen and Holst (1995) present the basis for grey-box modelling of the heat dynamics of buildings. A two-state model is fitted to data and maximum likelihood parameter estimation is carried out. Furthermore the relation between the continuous and discrete time representation is outlined, by rewriting the continuous time representation into a transfer function representation, i.e. an ARMAX model. The steady-state properties of the model are also described, i.e. how to obtain the estimated  $H$ -value of the building. Finally, the techniques for model evaluation are presented.

Andersen et al. (2000) model a residential test house divided into two test rooms with a water based central heating. A four-state model is applied, where the indoor and floor temperature of the two rooms are each represented separately with a state. Heat transfer coefficients and capacities and effective window areas in the lumped model are estimated. The model is validated both from a physical and statistical perspective.

Jiménez and Madsen (2008) present models for describing the thermal characteristics of building components based on data from in situ measuring. It is shown how the range from the most general non-linear stochastic grey-box model formulation to discrete transfer function models (ARMAX, black-box) over to linear regression models (steady-state models, i.e. no description of the dynamics) are related.

Bacher and Madsen (2011) present a procedure for selection of a suitable grey-box model for the heat dynamics of buildings. The suggested procedure is a forward model selection approach based on likelihood-ratio tests. It is demonstrated on five-minutes data from a 120 m<sup>2</sup> test building and a four-state model is identified as the most suitable model. In the procedure it is described how the models should be evaluated both from a physical and statistical perspective.

Lodi et al. (2012) presents grey-box modelling of a double skin building integrated photovoltaic system. The experimental data originates from tests carried out with an air-based system installed in a test reference environment. Both one-state and two-state non-linear grey-box models are considered. The most important energy performance parameters are estimated and the results are validated and discussed in detail.

Bondy and Parvizi (2012) present multi-room grey-box model of the heat dynamics of a building. Seven rooms in a 120 m<sup>2</sup>-building are modelled having two temperature states for each room and the heat transfers to the adjacent rooms. The indoor air temperature in each room is included in the model output and all parameters are estimated. The results are thoroughly evaluated concluding that they are in accordance with previous (simpler) studies of the building, prior physical knowledge and with the statistical assumptions.

## 7.5 References

1. Andersen K.K., H. Madsen, and L.H. Hansen. 2000. Modelling the heat dynamics of a building using stochastic differential equations. *Energy and Buildings*, 31(1):13–24.
2. Bacher P. and H. Madsen. 2010. Experiments and data for building energy performance analysis: Financed by the danish electricity saving trust. Technical report, DTU Informatics, Building 321, Kgs. Lyngby.
3. Bacher P. and H. Madsen. 2011. Identifying suitable models for the heat dynamics of buildings. *Energy & Buildings*, 43(7):1511–1522.
4. Bohlin T. and S.F. Graebe. 1995. Issues in non-linear stochastic grey box identification. *International Journal of Adaptive Control and Signal Processing*, 9(6):465–490.
5. Bondy D.E.M. and J. Parvizi. 2012. Modelling, identification and control for heat dynamics of buildings using robust economic model predictive control. Master's thesis, DTU.
6. Godfrey K.R.. 1980. Correlation methods. *Automatica*, 16(5):527–534.
7. Jazwinski A.H.. *Stochastic process and filtering theory*. Academic Press, New York, 1970.
8. Jiménez M.J. and H. Madsen. 2008. Models for describing the thermal characteristics of building components. *Building and Environment*, 43(2):152–162.
9. Jiménez M.J., H. Madsen, and K.K. Andersen. 2008. Identification of the main thermal characteristics of building components using matlab. *Building and Environment*, 43(2):170–180.
10. Kristensen N.R. and H. Madsen. 2003. Continuous time stochastic modelling, CTSM 2.3 - mathematics guide. Technical report, DTU.
11. Kristensen N.R., H. Madsen, and S.B. Jørgensen. 2004a. Parameter estimation in stochastic grey-box models. *Automatica*, 40(2):225 – 237.
12. Kristensen N.R., H. Madsen, and S.B. Jørgensen. 2004b. A method for systematic improvement of stochastic grey-box models. *Computers & Chemical Engineering*, 28(8):1431 – 1449.
13. Ljung L.. *System identification*. Wiley Online Library, 1999.
14. Lodi C., P. Bacher, J. Cipriano, and H. Madsen. 2012. Modelling the heat dynamics of a monitored test reference environment for building integrated photovoltaic systems using stochastic differential equations. *Energy & Buildings*, 50:273–281.

15. Madsen H. and J. Holst. 1995. Estimation of continuous-time models for the heat dynamics of a building. *Energy and Buildings*, 22(1):67–79.
16. Madsen H. and P. Thyregod. *Introduction to General and Generalized Linear Models*. CRC Press, 2010.
17. Madsen H. and J. Holst. *Modelling Non-Linear and Non-Stationary Time Series*. IMM, DTU, 2000.

